Bachelor Thesis

University of Bayreuth

Department Micrometeorology

Dynamics of the wind boundary layer profile and surface parameters at the Schneeberg summit in the Fichtelgebirge Mountains

Author: Sarah HOLDEN
Supervisor: Prof. Christoph THOMAS

November 28, 2016

Declaration of Authorship

I herewith certify that the work presented in the following with the title

"Dynamics of the wind boundary layer profile and surface parameters at the Schneeberg summit in the Fichtelgebirge Mountains" is to the best of my knowledge and belief original and the result of my own investigations. Third party work, non-published and published information I received are properly and duly acknowledged.

This work has never previously been submitted to any other examination committee.

Place, Date	Sarah Holden

Abstract

This work presents a 2 month meteorological research of the atmospheric boundary layer on the Schneeberg in the Fichtelgebirge Mountains. The data was collected by acoustic remote sensing with a Doppler Sodar. Data was retrieved in 98 height starting from $10\,[\text{meters}]$ to $495\,[\text{meters}]$ with a $5\,[\text{meter}]$ height resolution. By investigating the parameters wind direction, velocity, standard deviation of the vertical wind and wind direction difference, a wind profile for these heights was created and dominant wind flow regimes were defined. Special emphasis was placed upon the difference between Day and Night to detect a possible decoupling of wind systems in the valley and the mountain top.

The results show that the dominant wind direction is West-Southwest and wind velocities in a range of $7\,[\text{ms}^{-1}]$ to $8\,[\text{ms}^{-1}]$ were common. The σ_W is usually around $0.3\,[\text{ms}^{-1}]$ and $0.7\,[\text{ms}^{-1}]$ and the differences mostly under $50\,[°]$. Significant changes, which would indicate a decoupling of wind systems, could not be detected.

Zusammenfassung

Diese Arbeit umfasst eine zweimonatige Untersuchung der atmosphärischen Grenzschicht des Schneebergs im Fichtelgebirge. Die Datenaufnahme wurde mithilfe akustischer Fernerkundung mit einem Doppler Sodar erfasst. Der Datensatz beinhalten 98 Höhen, beginnend auf 10 [m] bis zu 495 [m] Höhe, mit einer 5 [m] Auflösung. Durch die Untersuchung der Parameter Windrichtung, Windgeschwindigkeit, Standardabweichung des Vertikalwindes und Windrichtungsunterschiede, konnten Windprofile für diese Höhen erstellt und dominante Windflüsse erkannt werden. Besonders die Unterschiede zwischen Tag und Nacht wurden hervorgehoben, um eine mögliche Entkopplung der Windsysteme im Tal und auf der Bergspitze, erkennen zu können.

Die Ergebnisse zeigen, dass die dominante Windrichtung west-südwest ist und Windgeschwindigkeiten gewöhnlicherweise zwischen $7\,[\mathrm{ms}^{-1}]$ und $8\,[\mathrm{ms}^{-1}]$ vorkommen. Das σ_W lag meist zwischen $0.3\,[\mathrm{ms}^{-1}]$ und $0.7\,[\mathrm{ms}^{-1}]$ und die Windrichtungsunterschiede unter $50\,[°]$. Es konnten keine wesentlichen Unterschiede dieser Parameter erkannt werden, die auf eine Entkopplung deuten würden.

Acknowledgement

This work could not have been possible without the great support of the working group 'Micrometeorology' and all its members, especially my supervisor Christoph Thomas. Constant help in expertise and encouragement were the heart and motivation of this time of research. Special thanks also to Andreas Held and his assistance. A great thanks particularly to Jo and his technical know-how and patience with our not so technical know-how. The other Joe who has also influenced this work is not any less to be mentioned. With his R-xpertise and English spirit he managed to "put the element of fun in every job that needed to be done". Also a special thanks to my dear friends Jonathan with his extensive help in the matter of "prettying up" this work with Latex, and Sophia and Hanna for advancing to masters of pep talks. Janice the menace and Groovie Rouvi deserve mentioning, for enduring those phone calls and Glashaus breaks.

Last but not least I want to give a heartfelt thank you to my loyal companion Elena. Without her support and more so friendship, this time would not have been the same in any way.

Contents

List of Figures

List of Tables

Introduction

Planet Earth is a system that oscillates between balance and imbalance. Energy, the engine of it all, can neither be created nor destroyed. Rather it is simply transformed and transported, stored and set free. Energy is generally gained by solar radiation and lost by long wave emission. The atmosphere only absorbs a small amount of this energy, whereas the majority is stored in earth's ground and oceans. The ground and oceans themselves serve as heating plates, transferring this energy in the form of latent, ground and sensible heat fluxes to the atmosphere (Foken and Nappo, 2008). And more specifically – to the atmospheric boundary layer (ABL). This is the part of the atmosphere which is the object of this research. The depth of the ABL can vary between $100\,\text{m}$ to $3000\,\text{m}$ (Stull, 1988). These very first meters are part of the troposphere. The troposphere is divided into the ABL and the free atmosphere and spans about $11\,[\text{km}]$ (Stull, 2005). This layer is where life and weather, as we know it, occurs. It is needless to say, that fundamental knowledge of the atmospheric boundary layer is crucial when investigating the interactions between atmosphere and biosphere.

Just as human life is defined by the atmosphere, so is the atmosphere defined by human life. The dynamic movement of air parcels is dominated by permanent change and pollution, which have almost an immediate effect (Stull, 1988). The need for current recording of the amount of greenhouse gases and its trends led to the founding of the national European network ICOs RI in 2008. ICOS RI (Integrated Carbon Observation System Research Infrastructure) provides scientific data about CO_2, CH_4, CO and radiocarbon – CO_2. To gather data, tall towers were built in several places in Europe such as the Ochsenkopf, Tušimice and Křesín. Whereas the latter ones are in the Czech Republic, the Ochsenkopf is located in Northern Bavaria. The measurements for this work will be conducted on the Schneeberg, which is a $1040\,[\text{m}]$ tall mountain, in close proximity of these locations.

This paper will investigate typical movements of air and structures of the ABL. These include turbulence due to surface roughness and heat fluxes. The ABL is, as mentioned above, very variable both in time and space. Figure 0.1 shows the typical diurnal evolution of the ABL.

With sunrise, incoming shortwave radiation heats the grounds and is transported to the atmosphere. The mixed layer grows and clouds can form. The heated air moves upwards, cools, and sinks again. At sunset, incoming energy ceases and the air cools down. Due to density differences, the air sinks and typically follows the slope of local topography to build cold air pools as so called cold-air drainage. This is the Stable Boundary layer and is present at night times. The Stable Boundary Layer is of lower magnitude than the mixed layer. The Residual Layer, also present at night, is a Layer of weak turbulence that confines the Stable Boundary Layer and is itself refined by the capping inversion. With sunrise the cycle begins anew. Inversions usually present in the mornings are dissolved by the heat fluxes coming from the warming grounds (Stull, 1988).

The Mountain top however is not dominated by this inversion dynamics. Due to the
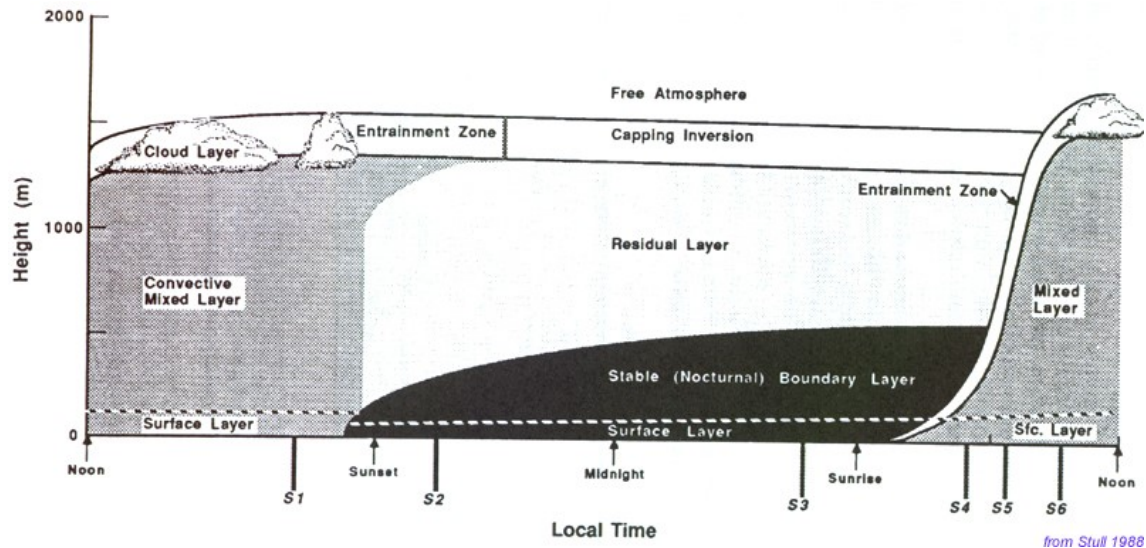
Figure 0.1: Typical diurnal evolution of the atmospheric boundary layer

higher elevation it is rather influenced by horizontal wind components. The effect of local topography, on the wind system of the Mountain top, increases with submesoscale winds and decreases with synoptic winds.

Especially relevant for this work are the transition times of night and day. During night, the cold-air drainage could lead to a decoupling of the wind systems on the top of the mountain and in the valley. Above this system, there is the free atmosphere. Because of the height of the Schneeberg $(1040\,[\mathrm{m}])$, it could be in the range of the free atmosphere. Whereas the wind system within the ABL is dominated by small-scale pressure gradients (mostly vertical winds due to convective movement), the system above this layer is rather influenced by synoptic systems, therefore the winds are expected to be horizontal. The partner experiment in the valley Voitsumra $(640\,[\mathrm{m}]$ above sea level) conducted research mainly focusing on inversion dynamics and temperature profiles, especially at night, and valley – mountain wind systems. Figure 0.2 shows the two sites in combination with the layer depth of a typical ABL.

The analysis on the Schneeberg focuses on dominating flow regimes both during day and night. Wind flows that are perturbed by orography, like a mountain, are compressed which leads to increased velocities right on top of the mountain. For a description of flows over mountain tops, the Froudesche Number is important. It describes the ratio between kinetic and potential energy. With an increase in potential energy (flow over mountain) the kinetic energy will increase (higher velocities).

If the $\mathrm{Fr} << 1$ the airflow is slow, if $\mathrm{Fr} >> 1$ the airflow is strong.

With the data of a Minisodar, chilled mirror and weather station, a first climatological profile is created at the Schneeberg.

To investigate the atmospheric boundary layer, it is most common to use remote sensing instruments, such as the Doppler SODAR used for this work. The research of John Tyndall layed the foundation for further development of SODARS. By using a foghorn over water, he detected scattering of sound through turbulence due to temperature and wind structure
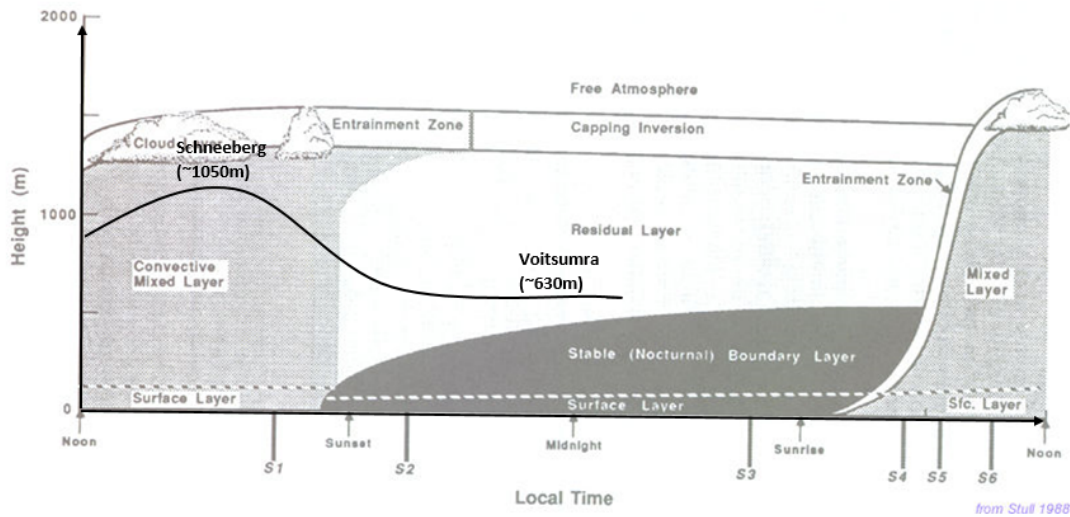
Figure 0.2: Heights of the Schneeberg and Voitsumra with the ABL structure

(Tyndall, 1874). This theory of acoustic backscatter was used by Gilman et al. for research of low-level temperature inversions. With his work he firstly introduced the acronym SODAR for 'Sounding Detection and Ranging' (Gilman, Coxhead, and Willis, 1946). This was followed by experimental research of the Russian scientist Kallistratova (Kallistratova, 1959) and the theoretical research of the Russian scientist Tatarski (Kallistratova and Tatarskii, 1960). Yet it was McAllister (McAllister, 1968) who applied these findings to several meters of height. He was the one introducing the sodargram which includes the dimensions of time and height. It was the research and measurements of Kelton and Bricout in 1964 that introduced the first SODAR systems based on the theory of the Doppler shift (Kelton and Bricout, 1964).This method was subsequently improved. Several works of Little should be mentioned in this matter (Little, 1969; Little, 1972b; Little, 1972a).

With this work the following objectives were pursued:

- Analyze the changes of the parameters wind velocity, wind direction, back scatter and σ_W with time and height
- Correlate relative humidity with aerosol measurements to detect fog events

1 Material

1.1 Minisodar

For this work the Scintec SFAS Minisodar was used. It emits and receives acoustic waves and provides a wind – height profile, retrieving data up to a height of 495 [m]. The Sodar consists of 64 antennas, an enclosure, a signal processing unit and power supply. It is a monostatic system. The antennas serve as both emitter and receiver. Figure 1.1 shows the antennas of the Sodar.

The measurements are conducted in cycles, with each cycle containing one to five subcycles. Each sub cycle emits in five different directions: E (East), W (West), V (Vertical), N (North) and S (South). The interval time for this experiment was 15 [min] with a maximum height of 495 [m]. The five different frequencies were 2548.9 [Hz], 2803.8 [Hz], 3058.7 [Hz], 3313.6 [Hz], and 3568.5 [Hz], with alternating tilted beams of 13.2 [°] and −7.9 [°]. Each Pulse is repeated 5 times.

1.1.1 Sodar Theory

The Sodar emits sound pulses which are scattered back by density inhomogenities. By means of the theory of the Doppler shift, a 3D-wind profile can be created. The Doppler shift describes the principle of a shift in frequency emitted and received due to a moving scattering medium. In the case of Sodar, there is a moving object (air parcels) and a stationary recipient (antenna). If the inhomogeneity in the air is moving towards the antenna, the frequency is compressed, if it is moving away it is stretched, leading to higher and lower received frequencies, respectively. The magnitude of the shift is calculated and wind speed profiles and Doppler images are created. For every image the wind components are determined and a 3D profile is developed.

$$V = \lambda \frac{\Delta f}{2}$$

With v = Doppler velocity, δf = Doppler frequency shift and λ = transmitted wavelength. Each measurement cycle provides raw data, which is processed to measured data

Figure 1.1: antennas of the Minisodar in the experiment set up

such as wind speed and wind direction.

1.2 Data output

The data derived by the Minisodar can be grouped into two general categories:

- Profile variables
- Non-profile variables

The profile variables are dependent of height and are provided for each height. Each dataset does therefore contain a complete height profile. Variables include wind speed and direction.The non-profile variables are independent of height, and include mixing height and stability class. The data are compiled in daily files. These typically contain 96 datasets of each 15 [min] of measurement for 500 [m] height with a 5 [m] resolution. The parameters significant for this work are wind speed in ms^{-1}, wind direction in degree, backscatter in db and σ_W in ms^{-1}.

1.3 Weather station

Additional to the Minisodar, a weather station was installed on the Schneeberg. The station contains a:

- Anemometer and wind vane
- Pyranometer
- Rain Gauge
- Relative Humidity and Thermohygrometer
- Chilled mirror

The wind anemometer and vane measure wind direction and wind speed, the pyranometer the magnitude of solar radiation and the rain gauge the amount of precipitation. The chilled mirror consists of a mirror and laser. If the relative humidity has reached 100 [%] there will be water drops condensing on the mirror and the laser beam, directed to the mirror, will be scattered. All in all the weather station will provide data to create a general meteorological profile of the Schneeberg.

1.4 Experimental site

The Schneeberg is 1064 [m] above sea level and is the tallest mountain in the Fichtelgebirge in the Northern of Bavaria. During the Cold War, it was used as a military base of Germany and the US Army. Therefore there are several buildings and a 80 [m] tall tower on the top of the Schneeberg. The experiment is installed on a roof of a two-story building, about 13 [m] distance to the tower. The roof is 7.18 [m] high. It has a second roof of 4.11 [m] height. The total size of the roof is about 37 [m] x 27 [m]. The Sodar is installed on the

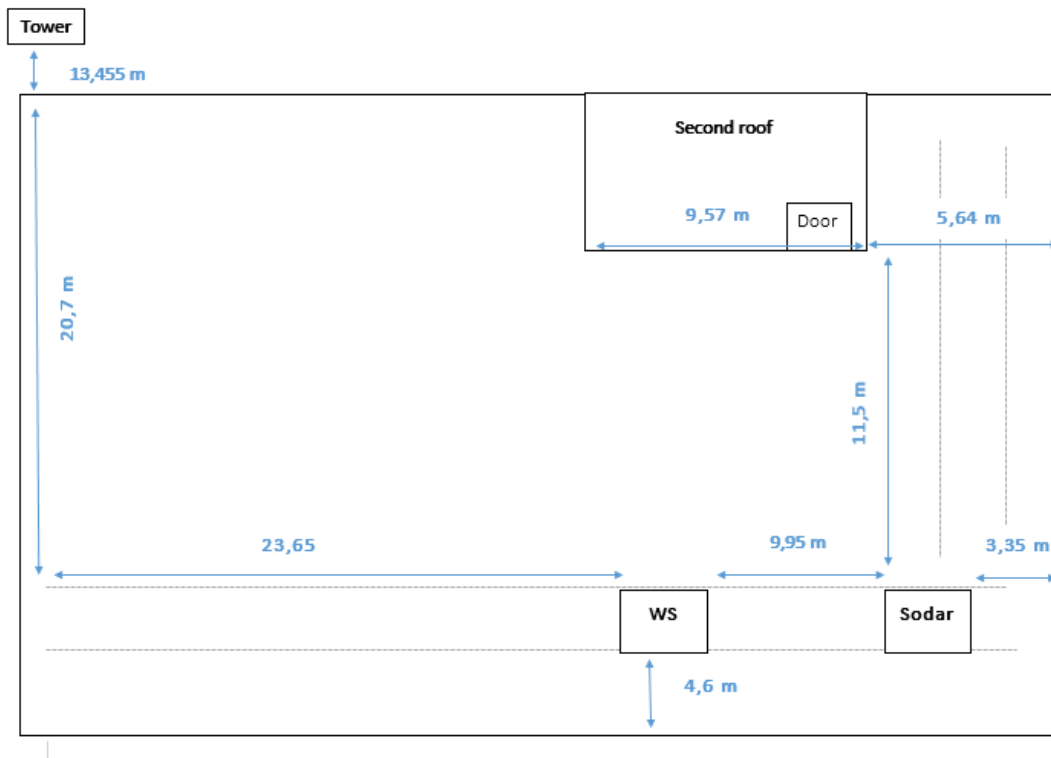Figure 1.2: technical drawing of the roof of the experiment set up

corner farthest from the tower. Figure 1.2 shows a technical drawing of the measurements of the experiment set up on the roof.

Figure 1.3 shows a map of the Fichtelgebirge with the Schneeberg and the distance to the Czech Republic and the tall tower in Tušimice as mentioned before.
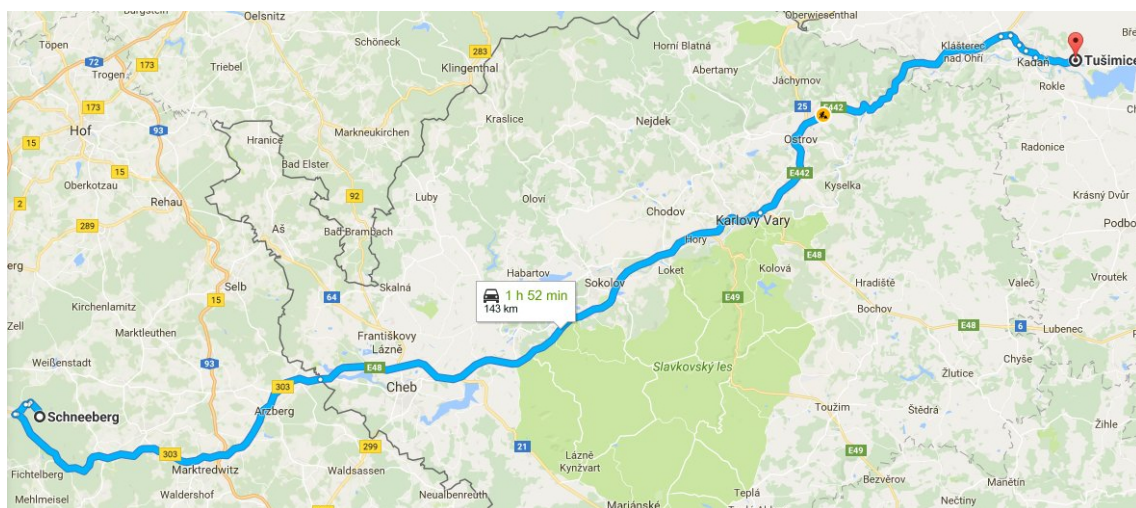
Figure 1.3: Distance of the Schneeberg to Tušimice in the Czech Republic

2 Methods

For the data evaluation the statistic program R was used. The relevant parameters wind speed, wind direction, backscatter and σ_W have already been calculated by the software program APRun 1.48. Figure 4.1 shows the schematic data flow of the software.

The measured raw data is preprocessed and filtered by Quality Control. For each parameters values of QC class, QC ignore and QC significance cumulative are created. The Quality Control is divided into 11 classes. The classes 10 and 11 are valid, all others invalid. Values which fall into invalid classes are marked as siC (low cumulative significance) or siD (low significance density) and are not included in the average. Thus values contaminated for example by ground clutter or low data density, are removed. The remaining values are the content of the main data files. The main data files are used for this analysis. These files include the values marked as invalid as well as assimilated and derived data. The output parameters relevant for the analysis of the climatological profile of the boundary layer of the Schneeberg are wind speed in ms^{-1}, wind direction in degree, back scatter in db and σ_W in ms^{-1}.

2.0.1 Classification of data

The data set consists of 41 data files, each representing one day in the measurement period of 01.07.2016 to 11.08.2016. Some days of measurement are incomplete due to data gaps and no data could be retrieved from the 15th of July. The measurements were conducted in 15 [min] intervals and up to a height of 495 [m] with a 5 [m] height resolution. Therefore there are 98 data points for each height. In this work however, the focus will be on the data height of 100 [m]. This reference is set just above the fixed echo seen in Figure 2.1. Table 2.1 and Table 2.2 show the density of data availability for 80 [m], 100 [m], 150 [m], 200 [m] and 250 [m]. 80 [m] has the highest data availability but because it is below the fixed echo and is therefore not representative, 100 [m] is used as the reference height.

Figure 2.1: Sodargram of backscatter

The data at 100 [m] shows a high density of available data and is just above the fixed echo seen in graph. The source of this fixed echo is probably the tower next to the roof, on which the measurements were conducted. However the data of other heights will be considered and included as a comparison with the reference, especially when analyzing wind differences at different height.

Table 2.1: Density distribution "Day"

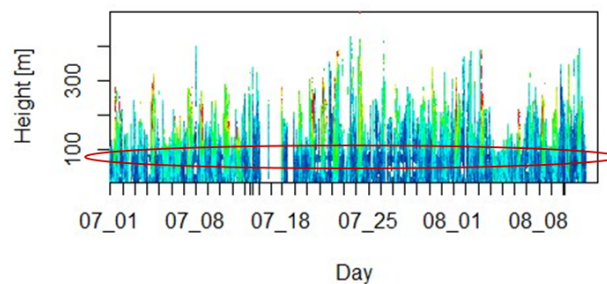|	80 [m]	100 [m]	150 [m]	200 [m]	250 [m]
Direction NAs day	96.00	130.00	254.00	520.00	915.00
Direction % day	94.60	92.68	85.71	70.74	48.51
Velocity NAs day	100.00	130.00	254.00	520.00	915.00
Velocity % day	94.37	92.68	85.71	70.74	48.51
Backscatter NAs day	110.00	201.00	478.00	1000.00	1477.00
Backscatter % day	93.81	88.69	73.10	43.73	16.88
sigma W NAs day	62.00	136.00	383.00	762.00	1145.00
sigma W % day	96.51	92.35	78.45	57.12	35.57

Table 2.2: Density distribution "Night"

	80 [m]	100 [m]	150 [m]	200 [m]
Direction NAs night	295.00	567.00	875.00	1201.00
Direction % night	83.40	68.09	50.76	32.41
Velocity NAs night	297.00	567.00	875.00	1201.00
Velocity % night	83.29	68.09	50.76	32.41
Backscatter NAs night	550.00	847.00	1230.00	1525.00
Backscatter % night	69.05	52.34	30.78	14.18
sigma W NAs night	25.00	309.00	736.00	1346.00
sigma W % night	98.59	82.61	58.58	24.25

The data at 100 [m] shows a high density of available data and is just above the fixed echo seen in graph. The source of this fixed echo is probably the tower next to the roof, on which the measurements were conducted. However the data of other heights will be considered and included as a comparison with the reference, especially when analyzing wind differences at different height. Due to suspected diurnal differences, the dataset was divided into "Day" and "Night" datasets. "Day" and "Night" are defined by data of the radiation measured by the weather station. The threshold value was set at $15\,[\text{W/m}^2]$. The mean of the time values which exceed this threshold define "Day" and the time values below define "Night". The time for sunrise was set at 7 am and the time for sunset at 7 pm. These "Day" and "Night" data sets were then used to create a climatological profile of the Schneeberg with the classifications explained above. Each phenomenon is examined for day and night separately.

2.0.2 Classification of cases

To distinguish typical flow regimes at the Schneeberg, some parameters were investigated more closely and compared. Table 2.3 shows the parameters and each's threshold value.

The division of day and night for these characteristics was a 12 hour time period starting from 7 am to 7 pm. These values are each defined by histograms, means and medians. The histograms are visualized for 100 [m] and 200 [m] above roof and the means and medians are for 100 [m] above roof, respectively.

These thresholds were applied to the data of the Schneeberg and three most common

Table 2.3: Classification table

Criteria	Classification	Indicator	
Wind direction WSW	Y = Yes	Day:	210 [°] - 290 [°]
	N = No	Night:	230 [°] - 320 [°]
Velocity	s = strong	Day:	Speed >7.2 [m/s]
	w = weak	Night:	Speed >7.9 [m/s]
Wind direction difference	h = high	Day:	Dif >16 [°]
	l = low	Night:	Dif >21 [°]
In all cases:	M = Mix		

cases were identified:

- YSL (West Southwest wind direction, strong winds and low direction difference)
- YML (West Southwest wind direction, mixed winds and low direction difference)
- YWL (West Southwest wind direction, weak winds and low direction difference)

2.0.3 Flowchart for classification

As shown in Table 2.3 there are three indications to specify each case. They are

- Wind direction
- Velocity
- Wind direction difference

Figure 2.2 shows a flowchart of the decision tree. D and N indicate Day or Night, respectively. Y, N or M indicate Yes, No or Mix of the dominant wind direction of west-southwest. Yes shows that this direction was present, No if not and Mix if a 2/3 majority cannot be reached for each criteria. The same scheme is applied for velocity. Also the wind direction difference is evaluated by low, high or Mix. With these classes, 54 cases are possible. These and the number of days and nights these cases occur are put together in Table 2.4 for "Day" and in Table 2.5 for "Night".

2.0.4 Wind direction

Figure 2.3 show the distribution of wind directions at a height of 100 [m] and 200 [m] for each in general and day and night separately. Wind direction was classified into two classes: west-southwest and other. Based on these graphs, the threshold value for the dominant wind direction west-southwest was defined. The limits for "Day" are 210° to 290° and for "Night" 230° to 320°. If 2/3 of 48 possible times of the direction of one day falls within these limits it is marked as Y for Yes and if 2/3 are below it is N for No. If neither definition reaches 2/3 it was marked as M for mixed.
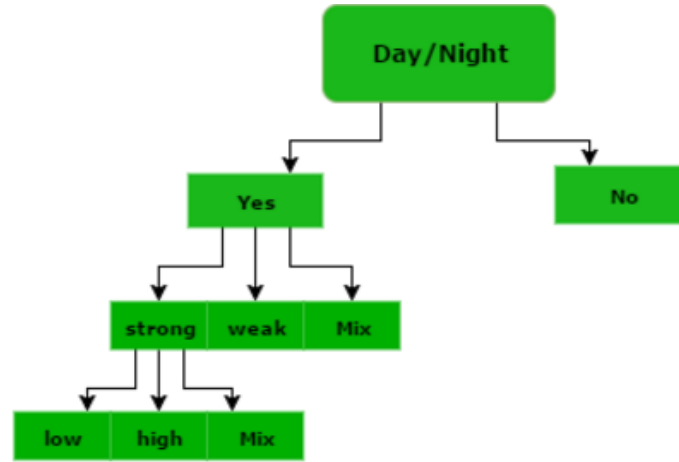
Figure 2.2: Flowchart for classification

Case	D/N	Dir	Vel	Dif	Occurences
1	D	Y	s	h	0
2	D	Y	s	l	11
3	D	Y	s	M	2
4	D	Y	w	h	0
5	D	Y	w	l	4
6	D	Y	w	M	0
7	D	Y	M	h	0
8	D	Y	M	l	4
9	D	Y	M	M	0
10	D	M	s	h	0
11	D	M	s	l	3
12	D	M	s	M	0
13	D	M	w	h	0
14	D	M	w	l	2
15	D	M	w	M	1
16	D	M	M	h	0
17	D	M	M	l	1
18	D	M	M	M	2
19	D	N	s	h	0
20	D	N	s	l	0
21	D	N	s	M	0
22	D	N	w	h	3
23	D	N	w	l	2
24	D	N	w	M	2
25	D	N	M	h	0
26	D	N	M	l	2
27	D	N	M	M	0
					$\sum$ 39

Table 2.4: Number of Days by Case

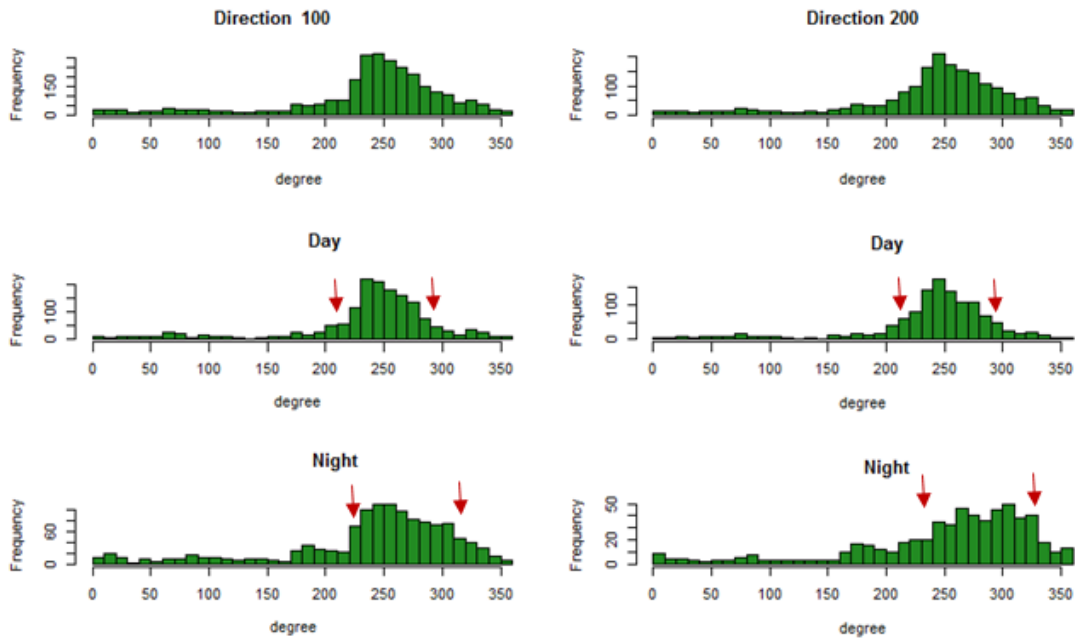| Case	D/N	Dir	Vel	Dif	Occurences
28	N	Y	s	h	1
29	N	Y	s	l	6
30	N	Y	s	M	1
31	N	Y	w	h	0
32	N	Y	w	l	4
33	N	Y	w	M	0
34	N	Y	M	h	0
35	N	Y	M	l	4
36	N	Y	M	M	3
37	N	M	s	h	0
38	N	M	s	l	2
39	N	M	s	M	0
40	N	M	w	h	0
41	N	M	w	l	2
42	N	M	w	M	2
43	N	M	M	h	0
44	N	M	M	l	0
45	N	M	M	M	2
46	N	N	s	h	0
47	N	N	s	l	2
48	N	N	s	M	0
49	N	N	w	h	3
50	N	N	w	l	2
51	N	N	w	M	3
52	N	N	M	h	0
53	N	N	M	l	0
54	N	N	M	M	3
					$\sum$ 40

Table 2.5: Number of Nights by Case

Figure 2.3: Distribution of wind direction at 100 [m] above roof (left) and 200 [m] above roof (right)

2.0.5 Velocity

For the classification of strong and weak winds, the median of "Day" and "Night" were used. The median velocity for 100 [m] during "Day" is 7.2 [ms^{-1}] and for "Night" 7.9 [ms^{-1}]. Figure 2.4 visualizes the distribution of wind velocity at the heights of 100 [m] and 200 [m] for each "Day" and "Night".

2.0.6 Wind direction Difference

The difference of wind direction with height was compared between 100 [m] and 200 [m].The comparison of the reference height 100 [m] and 200 [m] is interesting because, as Figure 2.7 and Figure 2.8 show, there is a clear shift of the wind direction at night.

Figure 2.5 and Figure 2.6 show the distributions of the direction difference in these heights. The mean wind direction difference for "Day" is 16 [°] and for "Night" 21 [°]. These represent the threshold value for high and low direction difference.

The references of 100 [m] and 200 [m] were chosen based on windroses as seen in Figure 2.7 and Figure 2.8. These show each day and night for the heights of 80 [m], 100 [m], 200 [m], and 250 [m]. There is a distinct wind direction change seen especially when comparing the 100 [m] and 200 [m] windroses.

2.0.7 Relative Humidity

The relative humidity was calculated by the dew point temperature of the chilled mirror. All data points equal to or above 100 [%] indicate fog days. Table 4.6 lists the amount of these occurences for "Day" and "Night", respectively.
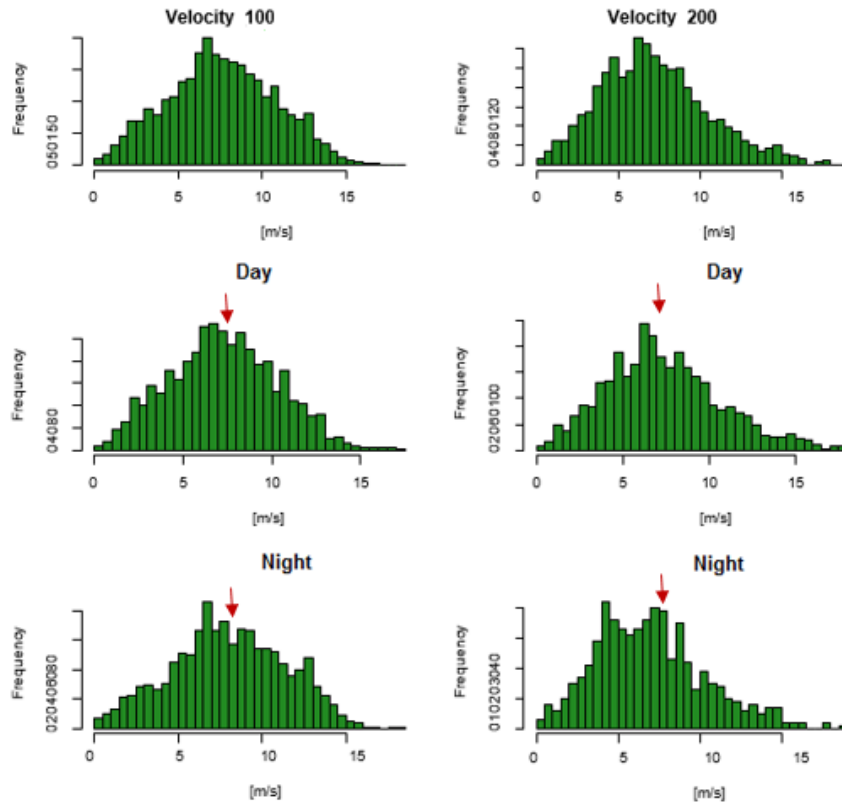
Figure 2.4: Distribution of wind velocity at 100 [m] above roof (left) and 200 [m] above roof (right)
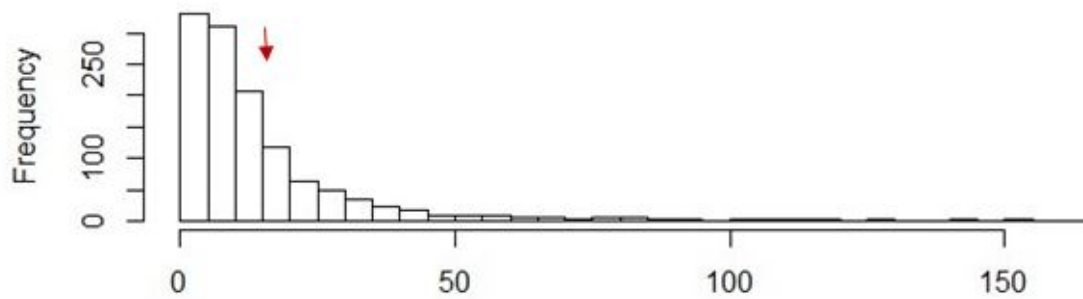
Figure 2.5: Distribution of direction differences during Day in °
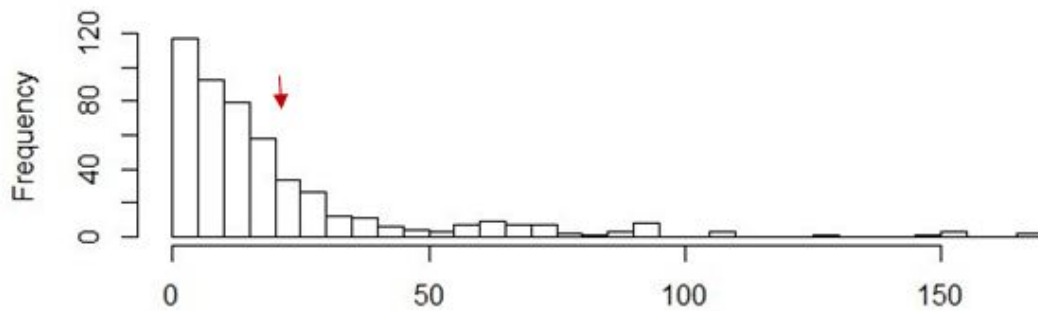
Figure 2.6: Distribution of direction differences during Night in degree

Figure 2.7: Windroses in $100\,[\mathrm{m}]$ (left) and $150\,[\mathrm{m}]$ (right) height for "Day" (top) and "Night" (bottom)

Figure 2.8: Windroses in 200 [m] (left) and 250 [m](right) height for "Day"(top) and "Night" (bottom)

3 Results

This classification into cases allow for creationing a climatological profile of the Schneeberg. The most common cases of combinations of wind direction, velocity and direction differences with height, of the measurement period are chosen and investigated more closely, by creating ensemble-averages of the values of the days of each case.

3.1 Mean wind climatology
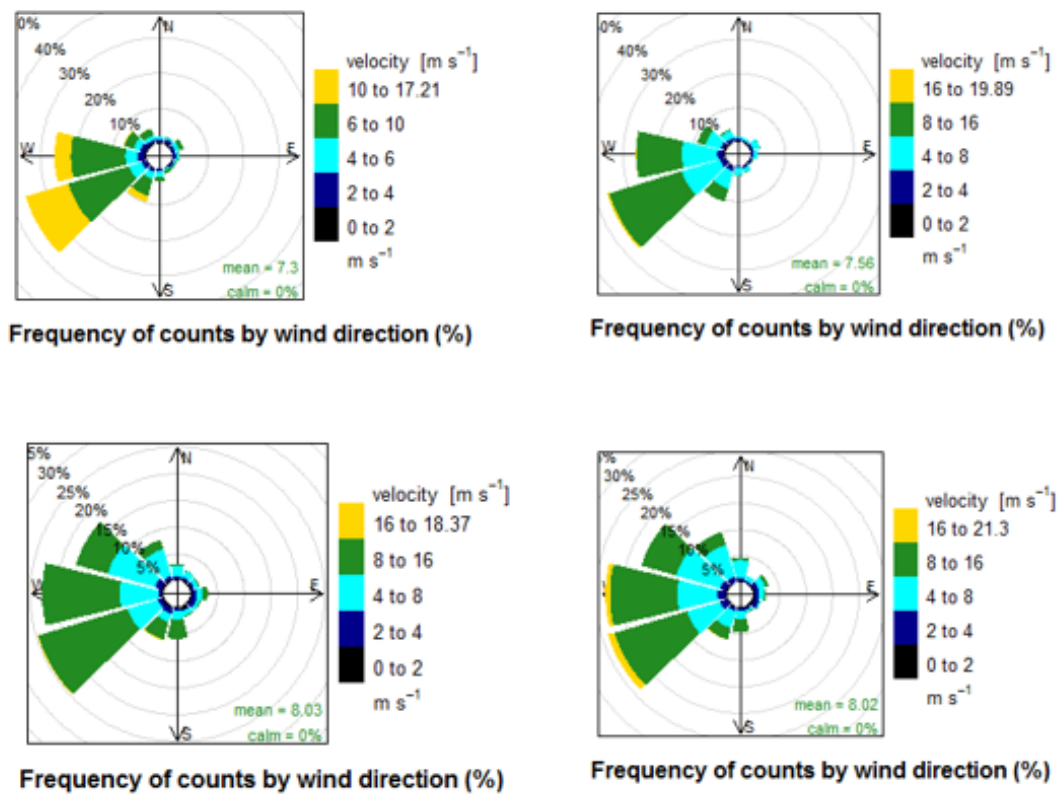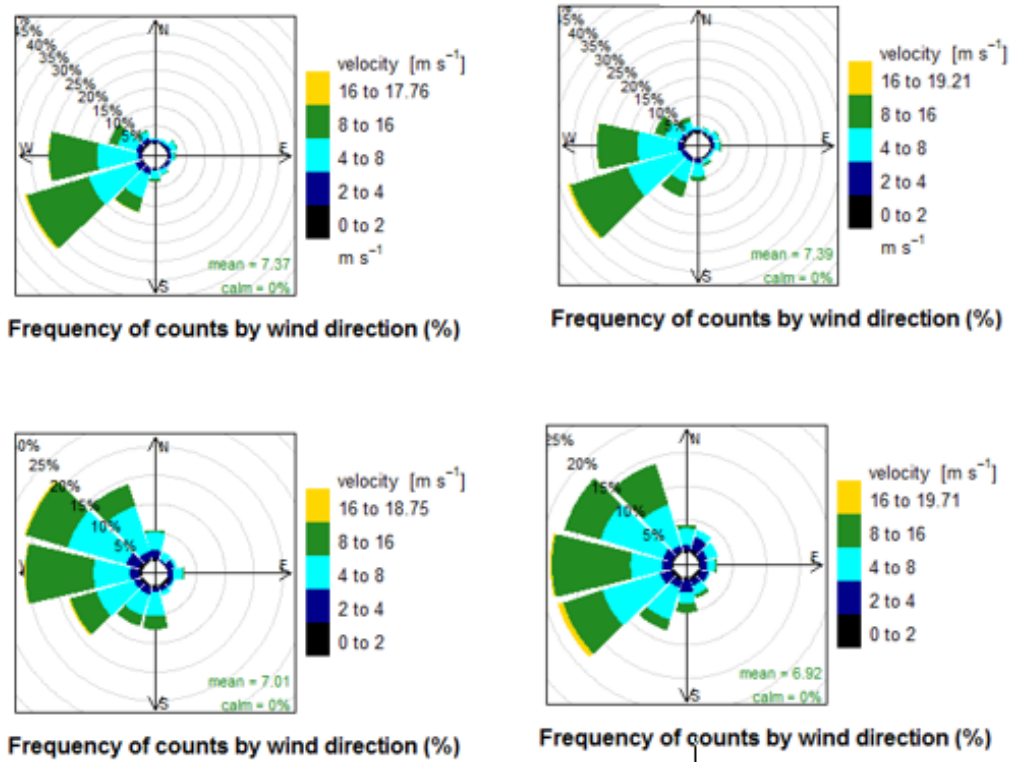
The mean wind speed for all 42 days between the hours of $7\,\mathrm{am}$ to $7\,\mathrm{pm}$ of $100\,[\mathrm{m}]$ height is $7.3\,[\mathrm{ms^{-1}}]$. The value for all nights between the hours of $7\,\mathrm{pm}$ to $7\,\mathrm{am}$ is $8\,[\mathrm{ms^{-1}}]$. In contrast to this the wind speeds for $200\,[\mathrm{m}]$ height are $7.3\,[\mathrm{ms^{-1}}]$ for days and $7\,[\mathrm{ms^{-1}}]$ for night. The winds in $100\,[\mathrm{m}]$ and $200\,[\mathrm{m}]$ height are mainly dominated by west-southwest winds. There is very little wind direction difference to be seen.

3.2 Wind direction

Figure 2.3 represents the distribution of wind direction in the heights of $100\,[\mathrm{m}]$, $150\,[\mathrm{m}]$, $200\,[\mathrm{m}]$, and $250\,[\mathrm{m}]$, each for day and night separately.

3.2.1 Windroses

Figure 2.7 and Figure 2.8 show a clear distinction of "Day" and "Night". During "Day" the wind direction is predominantly from the Southwest. During "Night" the amount of West and Northwest winds increase.

3.3 Wind velocity

The values for "Day" and "Night" of wind velocity differ very little. Figure 2.4 shows the distribution of velocity values in heights of $100\,[\mathrm{m}]$ and $200\,[\mathrm{m}]$ for "Day" and "Night".

3.4 sigma W

Table 3.1 shows the standard deviation of the vertical wind component of wind speed at 5 different heights.

3.5 Relative humidity and aerosol measurement

Figure 3.1 shows the trend of the relative humidity for the measurement period of 01.07. until 11.08.. There are several rain and or fog events present. The aerosol measurements were conducted in the time span of 05.07. until 20.07.. Three different sizes were analyzed.
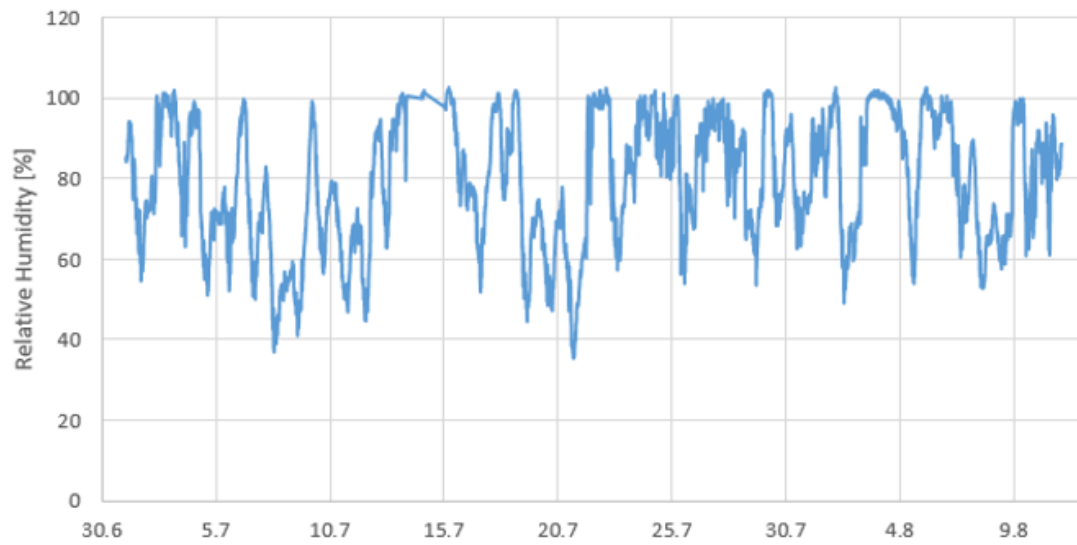
Figure 3.1: Trend of the relative humidity for the measurement period
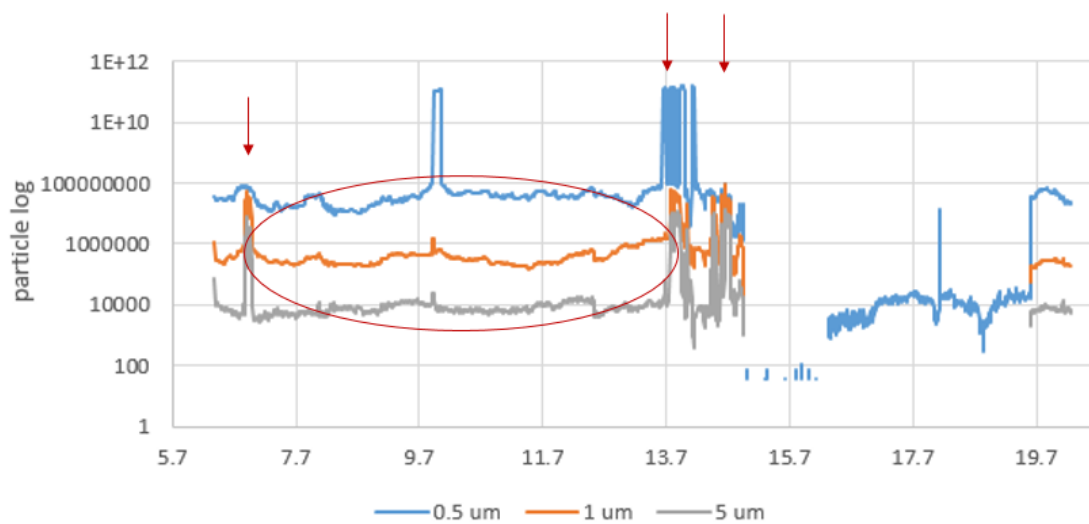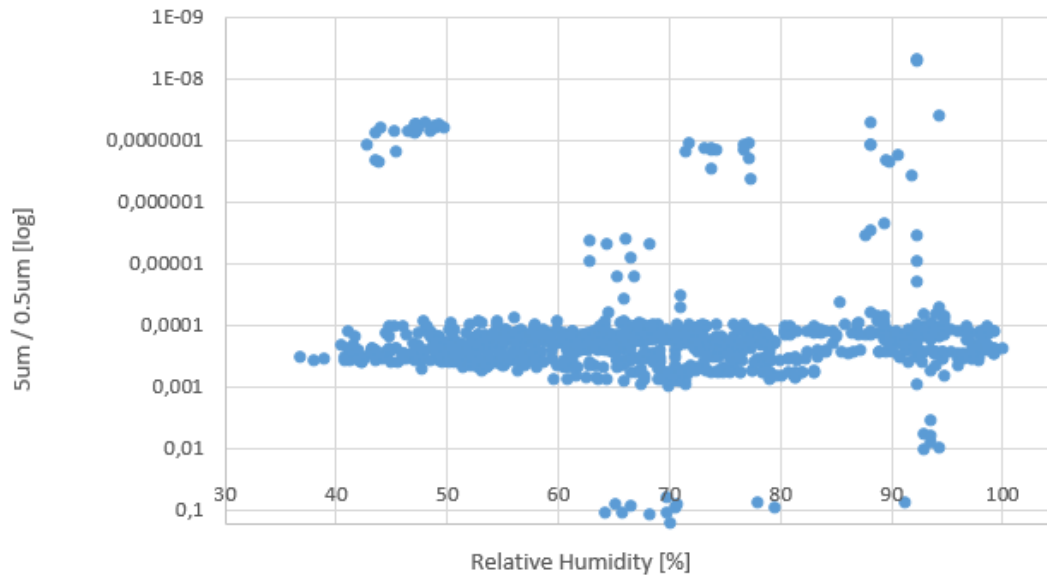

Figure 3.2: Time series of the three aerosol size measurements

Table 3.1: σ_W in ms -1 of height $80\,\text{m}$ to $250\,\text{m}$

Height [m]	σ_W [ms^{-1}]
80	0,33
100	0,43
150	0,55
200	0,67
250	0,77

Figure 3.3: Correlation of relative humidity and 5 [µm]: 0.5 [µm] ratio

0.5 [µm] in channel 1, 1 [µm] in channel 2, and 5 [µm] in channel 3, respectively. These are visualized in Figure 3.2

Figure 3.2 shows the different aerosol sizes. There are three cloud events to be seen on the 6th, the 13th and 14th of July, indicated with arrows. During the 14th and 16th of July there were technical difficulties. For further analysis of aerosol and relative humidity the time span of 6th and 12th of July will be looked at more closely.

Figure 3.3 shows the correlation of relative humidity with the 5 [µm] aerosols and 0.5 [µm] aerosols ratio. The majority of the measurements show no significant increase of bigger aerosols with increasing humidity. However there are several distinct cases which show a clear correlation of humidity increase and significant amount of bigger aerosols. The ratio of bigger and smaller aerosols is signficant because a high ratio would indicate a sudden increase in bigger aersosols which points to the growing of waterdrops and eventually clouds.

3.6 Cases

Table 2.4 and Table 2.5 show the occurrences of cases in the measurement period. The most common cases for day and night respectively are analyzed more closely below.
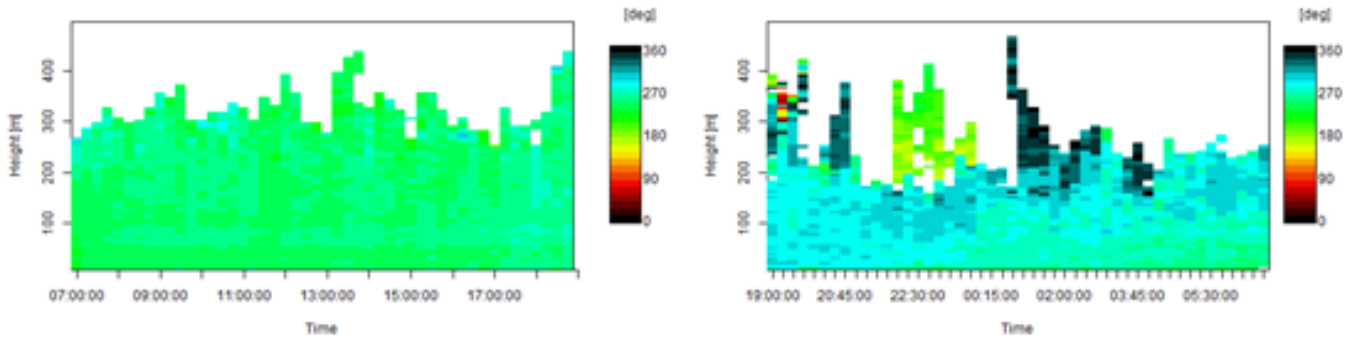
Figure 3.4: Sodargram of direction case YSL,left: "Day", right: "Night"

3.6.1 Case: YSL

The most common Case during "Day" and "Night" is YSL. It occurs on 11 of 39 days during"Day" and 6 of 40 nights of "Nights". This case represents

- Wind direction West southwest
- strong winds
- low σ_W

The sodargrams Figure 3.4 to Figure 3.11 show the means of wind direction, velocity, direction difference and σ_W of these days for "Day" and "Night". The profiles for each parameter show the means of the days for each height. Figure 3.4 and Figure 3.5 show that there is little variance of wind direction during day but slightly more during night.This is supported by Figure 3.8. There is higher wind direction difference to be seen above the first 150 [m]. The profiles show a clear consistency during "Day" and a clear increase during "Night" starting from 100 [m]. The direction in general is during "Day" predominantly west-southwest and at "Night" the west and even northwest component increase. The velocities in general decrease at "Night" and show a rather significant distinction of the first 100 [m] to velocities above. This distinction is also seen during "Day" but much lower which could be explained by higher pressure gradients and therefore higher velocities during "Day". The source for high pressure gradients is the discrepancy of low pressure on the grounds during day, due to rising warm air, and high pressures of accumulating cooler air masses above. This interpretation is supported by the standard deviation of vertical wind velocities in Figure 3.10 and Figure 3.11. If taken as an indicator for turbulence, it shows higher turbulence during "Day" than "Night". The standard deviation shows a diurnal cycle during "Day". During noon it is higher than in the evenings and mornings. This would mean lower turbulence in the mornings and evenings which is due to low or non existent thermally induced heat flows.

3.6.2 Case: YML

The Case YML occurs 4 times out of 39 days during "Day" and 4 times out of 40 during "Night". It represents

Figure 3.5: Profile of direction case YSL,left: "Day", right: "Night"

Figure 3.6: Sodargram of velocity case YSL, left: "Day", right: "Night"

Figure 3.7: Profile of velocity case YSL, left: "Day", right: "Night"

- wind direction west southwest
- neither strong nor weak winds
- low σ_W

The sodargrams Figure 3.12 to Figure 3.19 show the means of wind direction, velocity, direction difference and σ_W of these days for "Day" and "Night". The profiles for each parameter show the means of the days for each height. The wind direction in Figure 3.12

Figure 3.8: Sodargram of direction difference case YSL,left: "Day", right: "Night"

Figure 3.9: Profile of direction difference case YSL

Figure 3.10: Sodargram of σ_W case YSL,left: "Day", right: "Night"

Figure 3.11: Profile of σ_W case YSL,left: "Day", right: "Night"
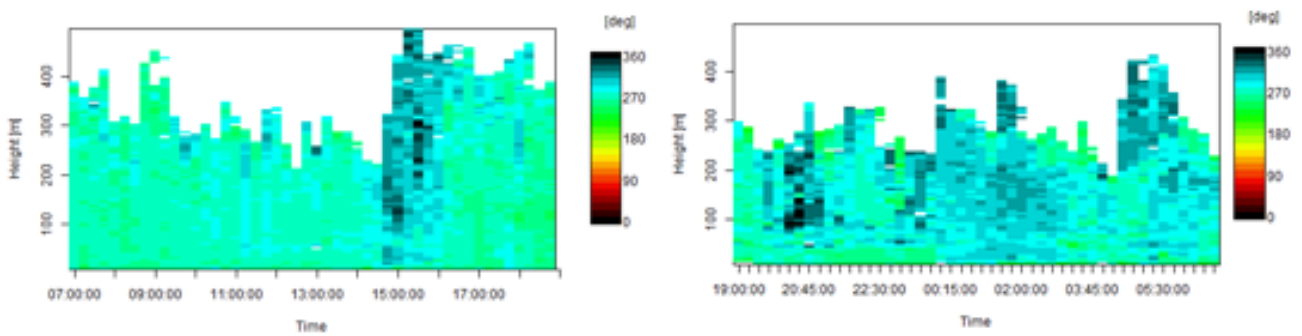
Figure 3.12: Sodargram of direction case YML,left:"Day", right:"Night"

and Figure 3.13 show just as in case "YSL" little variability during "Day" and also during
"Night". However the wind direction is dominated more by west winds. Little change is
seen to "Night". Interesting is the area of north winds around 15:00. Figure 3.14 shows
a similar change at that time to much lower wind speeds. A similar pattern is seen in
Figure 3.18. It shows higher turbulence in the first half of the days and then less in the
afternoon. This could be associated with cloud occurrence. Figure 3.15 at "Night" shows
an almost linear increase of wind speeds with height to up to 10 [m/s]. The difference in
wind direction is again insignificant. The profiles however show slightly higher differences
during "Night" than "Day". This is to be seen in all of the three cases and could be due
to cloud occurence. The standard deviations in Figure 3.18 shows an increase in the early
afternoon during "Day" and overall low values during "Night". Figure 3.19 shows the same
pattern and also a decrease of the standard deviation in a height of 200 [m] during "Day".

3.6.3 Case: YWL

The Case YML also occurs 4 times out of 39 days during "Day" and 4 times out of 40
during "Night". It represents

- wind direction west southwest
- weak winds
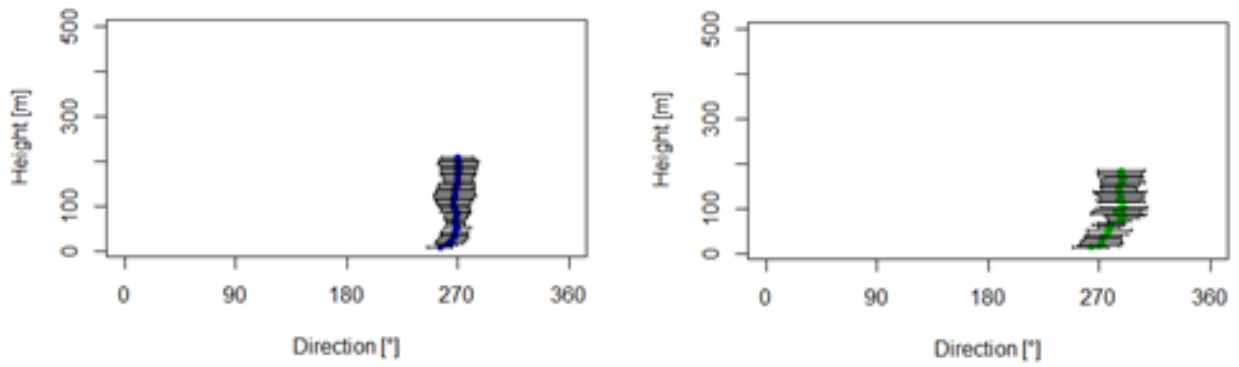
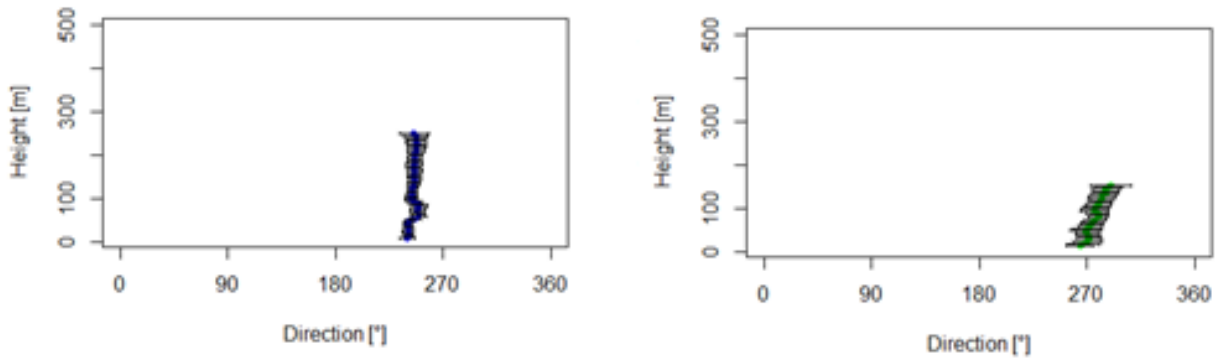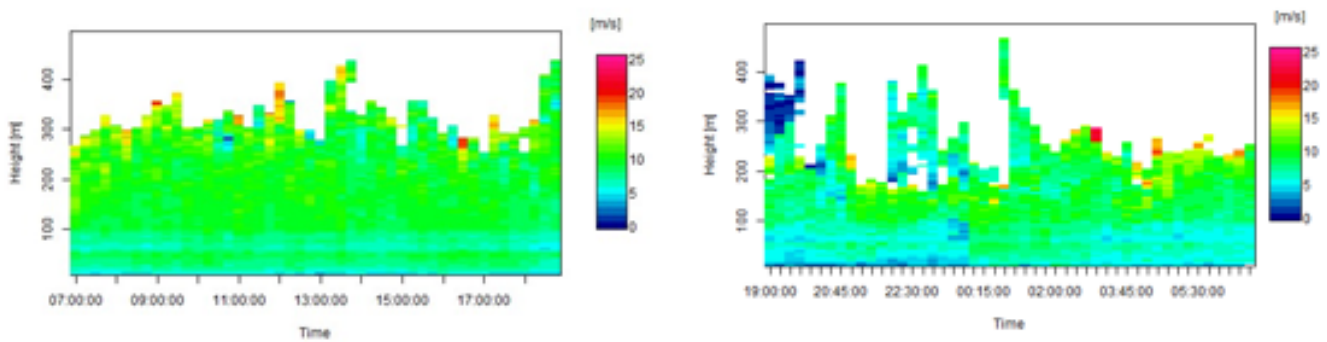Figure 3.13: Profile of direction case YML,left:"Day", right:"Night"
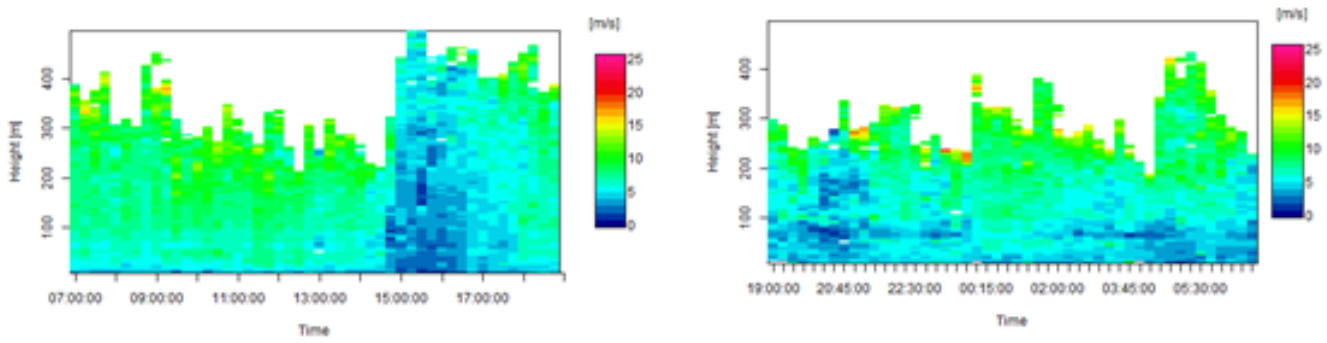
Figure 3.14: Sodargram of velocity case YML, left:"Day", right:"Night"

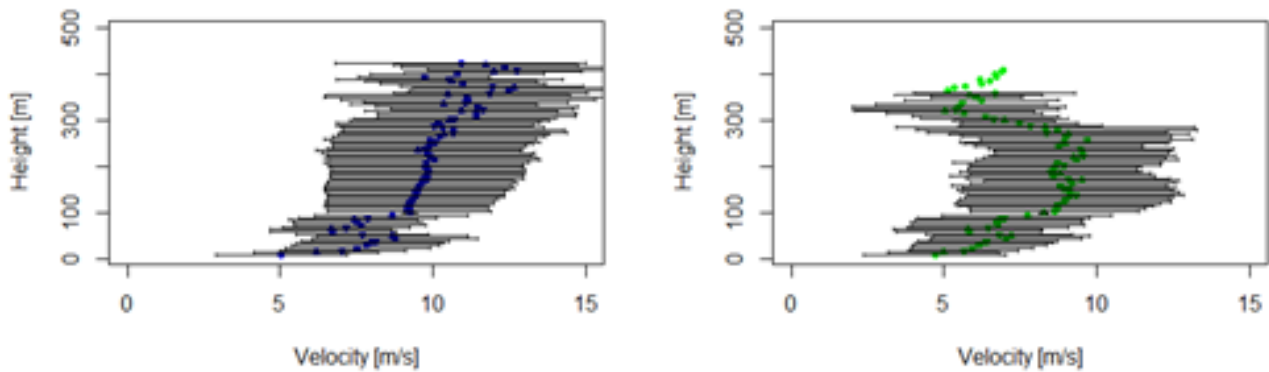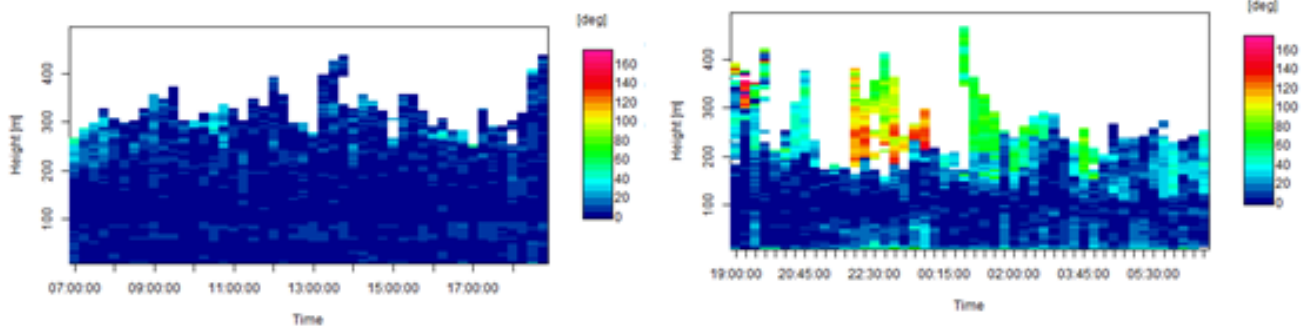Figure 3.15: Profile of velocity case YML, left:"Day", right:"Night"

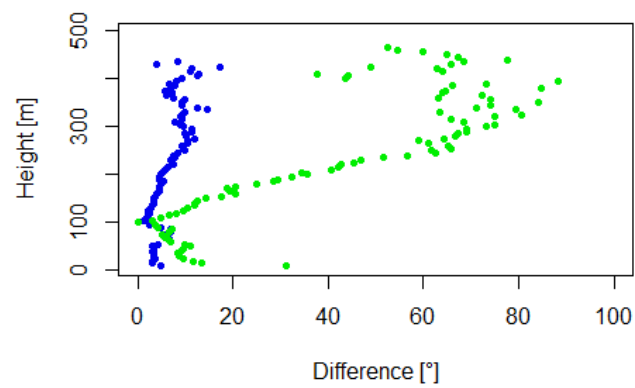Figure 3.16: Sodargram of direction difference case YML,left:"Day", right:"Night"

Figure 3.17: Profile of direction difference case YML
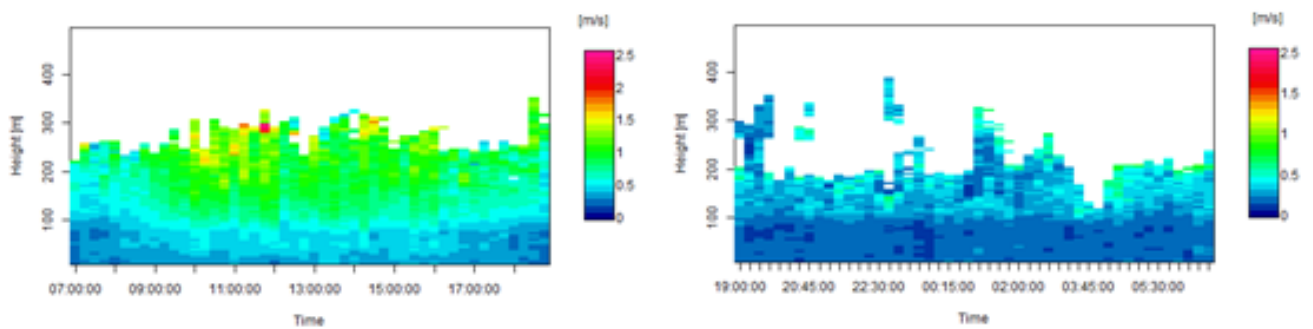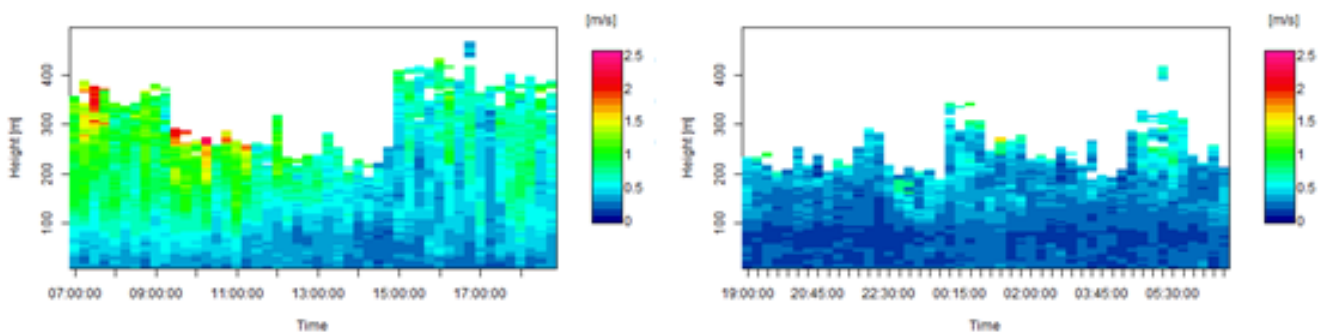

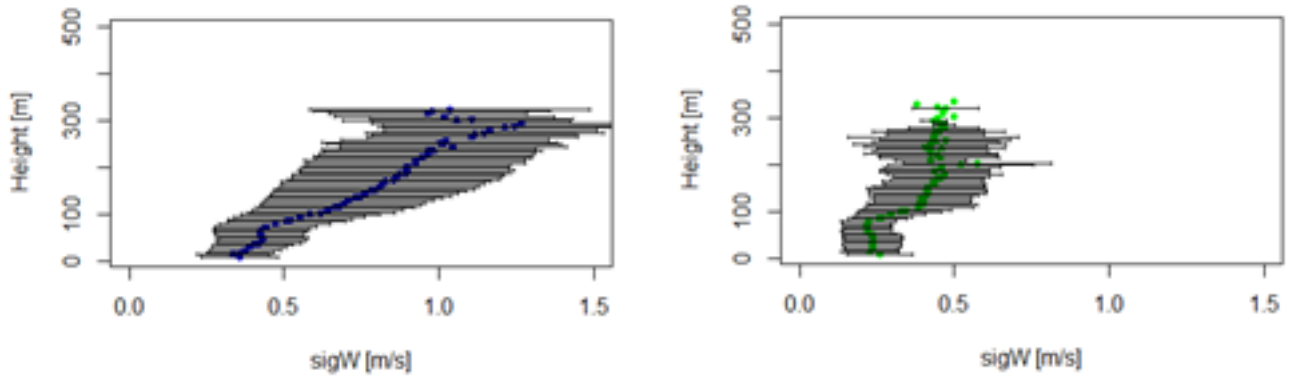Figure 3.18: Sodargram of σ_W case YML,left:"Day", right:"Night"

Figure 3.19: Profile of σ_W case YML,left:"Day", right:"Night"

Figure 3.20: Sodargram of direction case YWL,left:"Day", right:"Night"

- low σ_W

The sodargrams Figure 3.20 to Figure 3.27 show the means of wind direction, velocity, direction difference and σ_W of these days for "Day" and "Night". The profiles for each parameter show the means of the days for each height. This case is, compared to the others, one of a weak wind regime. The wind direction shows increased south winds during "Day" and significant variability during "Night". Figure 3.20 at "Night" shows strong changes from south-winds to west-winds. The profiles for direction show more or less constant west-wind directions during "Day" and rather west-winds during "Night". As this represents a low wind speed regime the velocities are lower compared to the cases "YSL" and "YML". Figure 3.23 shows a stronger increase of wind speeds with height during "Day". Again there is a slight distinction of lower and stronger winds at around 100 [m] height. Figure 3.26 shows a strong increase of turbulence with height during "Day". During "Night" the σ_W is rather small.
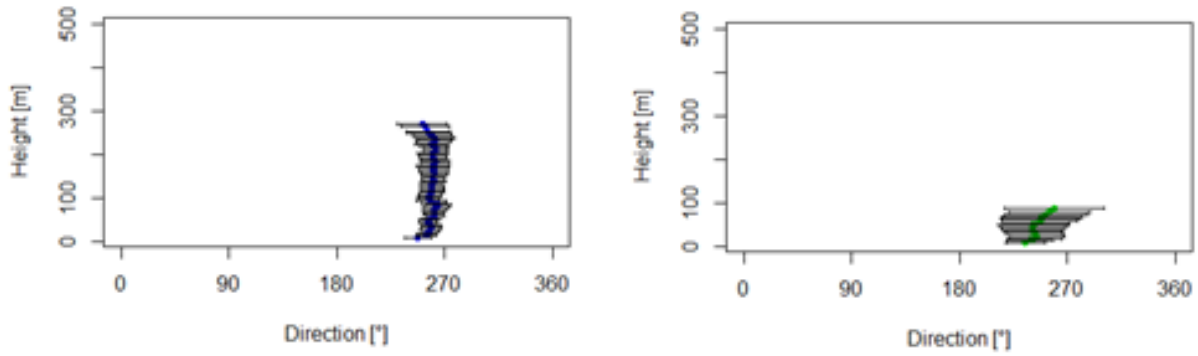
Figure 3.21: Profile of direction case YWL,left:"Day", right:"Night"
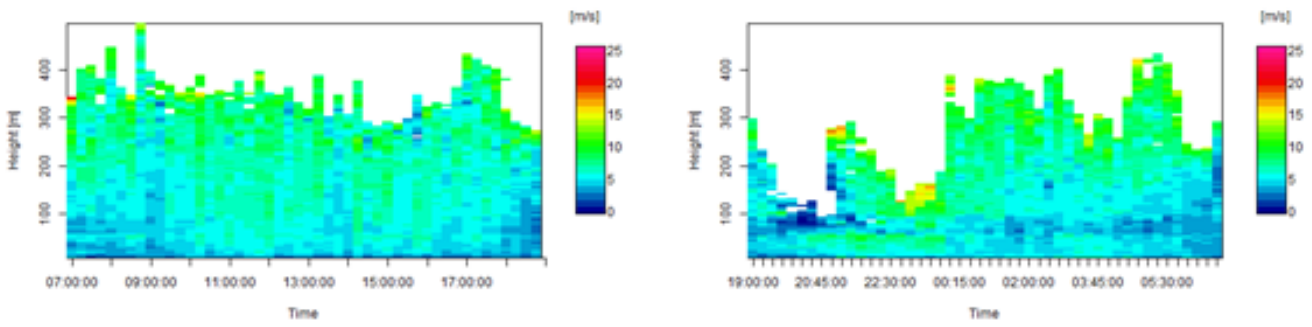
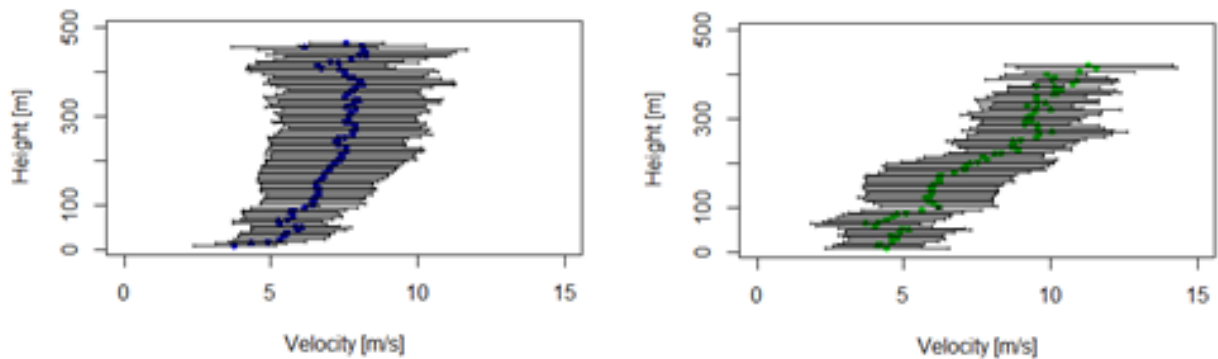Figure 3.22: Sodargram of velocity case YWL, left:"Day", right:"Night"
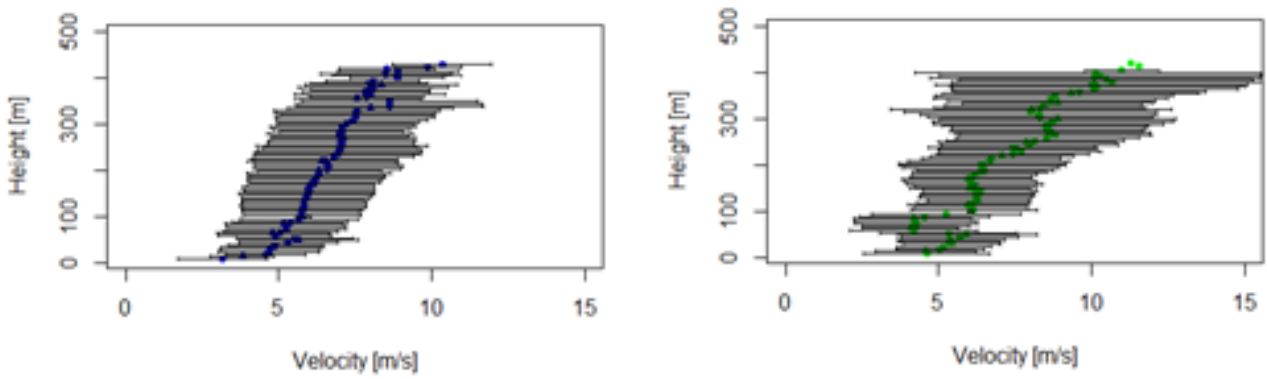
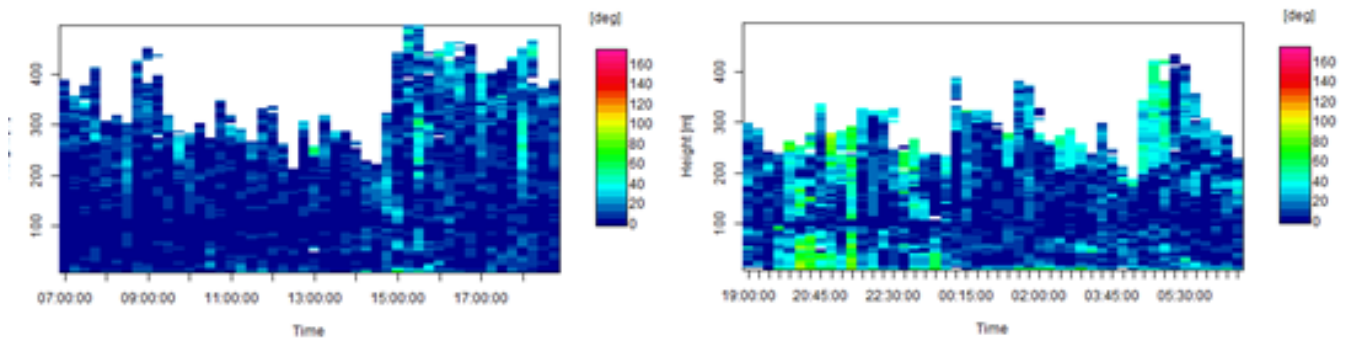Figure 3.23: Profile of velocity case YWL, left:"Day", right:"Night"
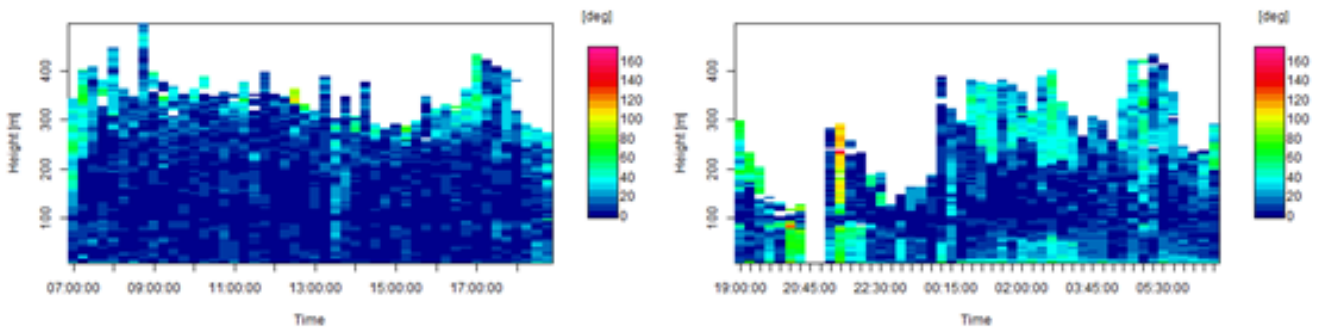
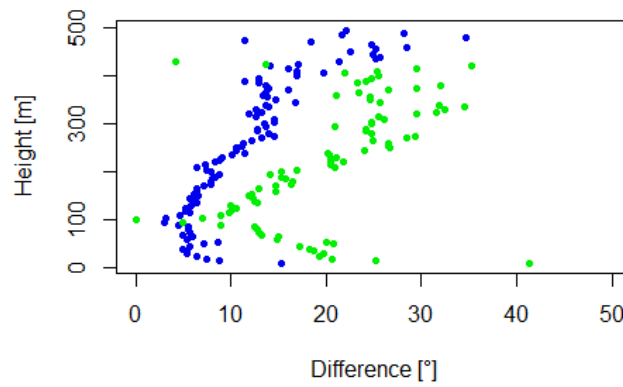Figure 3.24: Sodargram of direction difference case YWL,left:"Day", right:"Night"
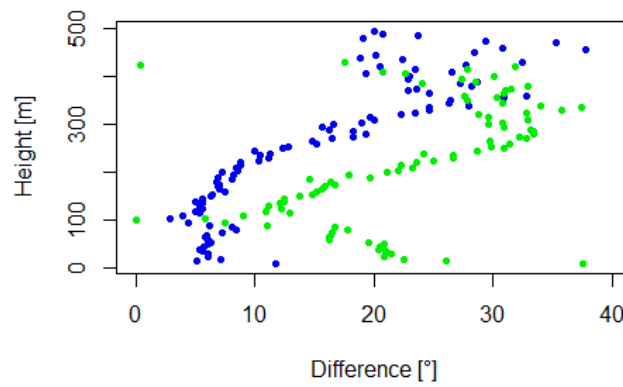

Figure 3.25: Profile of direction difference case YWL
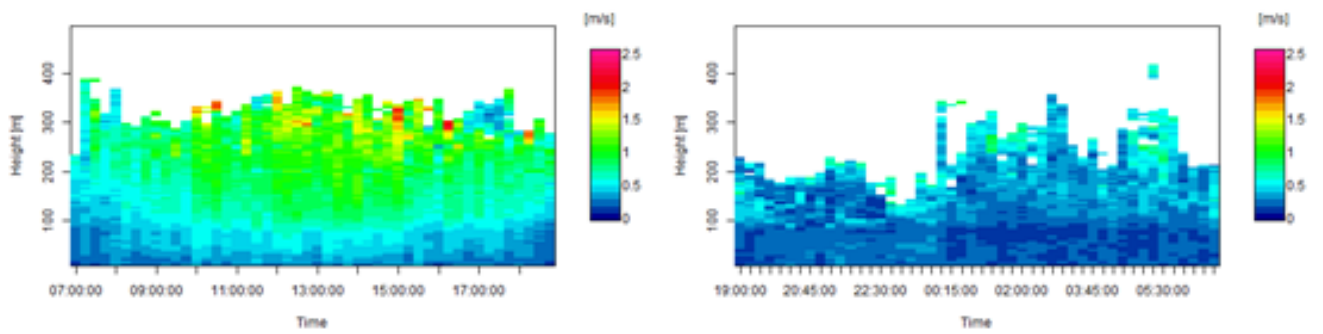
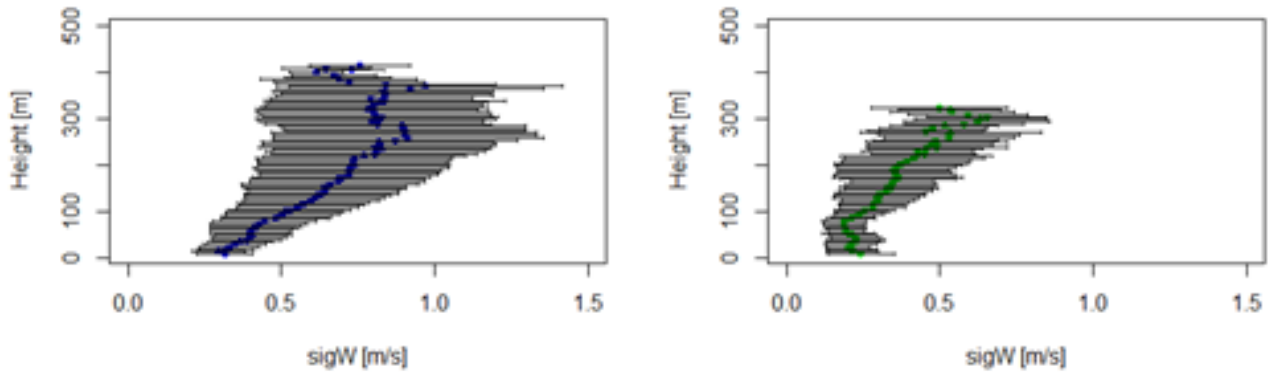Figure 3.26: Sodargram of σ_W case YWL,left:"Day", right:"Night"

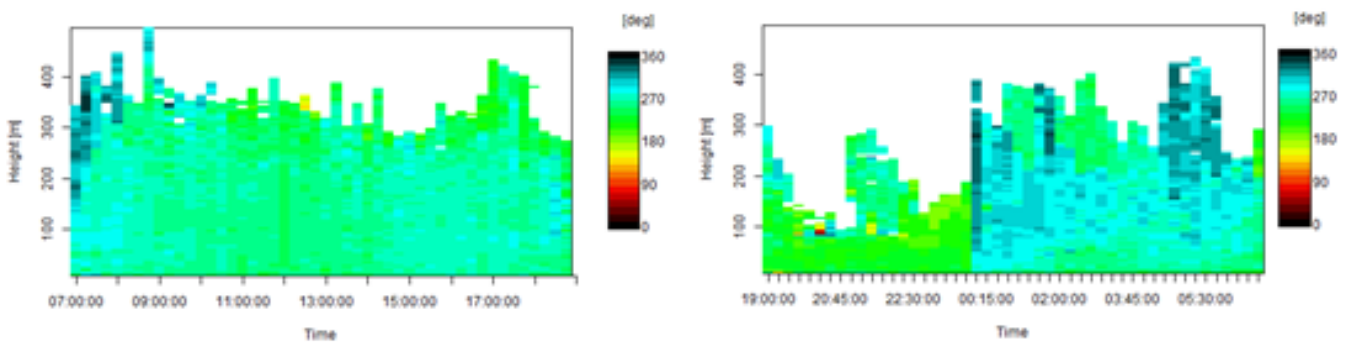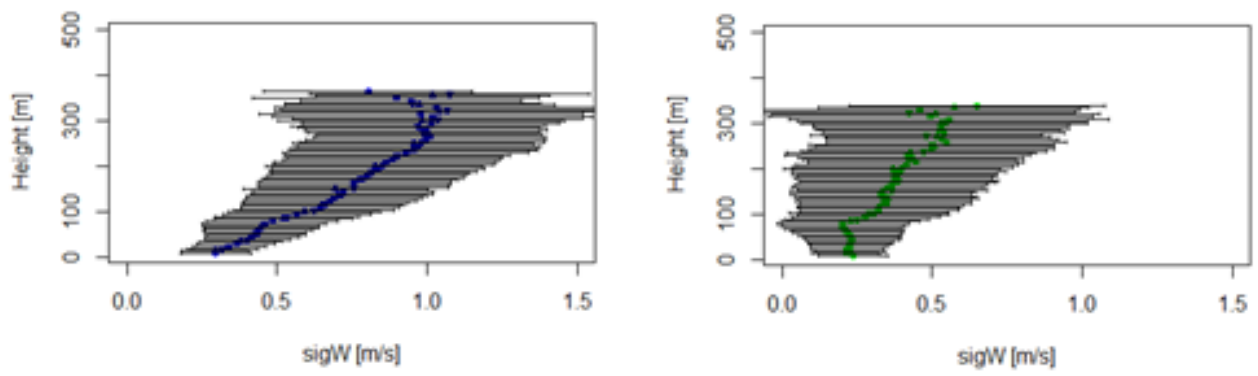Figure 3.27: Profile of σ_W case YWL,left:"Day", right:"Night"

4 Discussion

The methods to classify flow regimes were strongly influenced by the work of Jerilyn Walley. The work analyzed two adjoining valley sites in the Andrew Experimental Forest in Oregon. The criteria used for the classification were synoptic forcing, wind direction, presence of valley jets, pulsing of speed and direction and the similarity of phenomenons at both sites. It was concluded that the most important criteria were flow direction and valley jets (Walley, 2013).

However, the results of the Andrew Experimental forest rather apply to valleys than mountains. In their paper, W.-Y. Sun and O. M. Sun, 2015 describe the flow over mountains and its consequences for air parcels. In their theoretical approach, based on the Bernoulli equation, they conclude that a rising air parcel will experience an increase in kinetic energy (i.e. wind speed) at the peak of the mountain. However, in contrast to other explanations they credit this to a change in enthalpy rather than a change in potential energy. This can be seen in some of the ensemble-averages especially during night in the YSL case in Figure 3.6.

The hypothesis of this work was that the wind system of the mountain top and the valley would be decoupled especially during nights. The data of the Schneeberg and the valley Voitsumra were not compared however the data of the Schneeberg was analyzed in height and time. If the ABL would have sunk enough to expose the Schneeberg to the free atmosphere, the standard deviation, as a measure for turbuluence, would have decreased. Furthermore the velocity and wind direction would have shown very little variability. However, this could not be clearly seen.

There are only slight changes in velocity and σ_W when comparing day and night. These are probably more due to decreasing pressure gradients during the night, rather than an actual decoupling. It might be important to consider that the data was collected during a summer with above average temperature, which results in a strong convective layer and high pressure gradients. This coincides with a strong residual layer during night, which could have prevented the Schneeberg to be exposed to the free atmosphere. This dependence of the growth of the convective boundary layer to thermal induction is also shown in Kossmann et al., 1998. As part of the TRACT Experiment they collected data with radiosondes, tethered balloons, sodars, and other sounding systems to observe the ABL in the Rhine valley and in the Northern black forest. It was found that thermally induced up-slope winds have a strong influence on the CBL depth in complex terrains.

Conclusion

The results presented above depict a first idea of the meteorological profile of the Schnee-berg. With this research, general dominant wind regimes were detected. These were wind directions from West Southwest, strong winds in the range of $7 \, [\mathrm{ms}^{-1}]$ to $8 \, [\mathrm{ms}^{-1}]$ and low wind direction differences in $100 \, [\mathrm{m}]$ and $200 \, [\mathrm{m}]$. The standard deviation, as a factor for turbulence, is higher during day than night. As for the parameter of wind direction difference, no directional shear could be detected. This parameter could have been left out or the thresholds value should be adapted, to have more significant contributions.

The dominant wind direction of West Southwest makes sense as the weather in Germany is dominated by winds of the west wind zone. The Schneeberg is surronded by the Ochsenkopf ($1024 \, [\mathrm{m}]$) in the West Southwest and the Fichtelberg ($680 \, [\mathrm{m}]$) in the South. In the North there is the Weißenstädter Becken and in the East lies Wunsiedel ($525 \, [\mathrm{m}]$). The Meteorology on the Schneeberg is strongly influenced by this local topography of rather flat areas in the East and high ones in the West.

The measuring period of this research was too short to find significant results. A longer and maybe even interannual analysis could provide more meaningful data.

Bibliography

AG, Scintec (2016). "Software Manual". In:

Foken, T. and C.J. Nappo (2008). *Micrometeorology*. Springer Berlin Heidelberg. ISBN: 9783540746669.

Gilman, GW, HB Coxhead, and FH Willis (1946). "Reflection of sound signals in the troposphere". In: *The Journal of the Acoustical Society of America* 18.2, pp. 274–283.

Kallistratova, MA (1959). "Procedure for investigating sound scattering in the atmosphere". In: *Sov. Phys. Acoust* 5, pp. 512–514.

Kallistratova, MA and VI Tatarskii (1960). "Accounting for wind turbulence in the calculation of sound scattering in the atmosphere". In: *Sov. Phys. Acoust., Eng. Trans*, pp. 503–505.

Kelton, G and P Bricout (1964). "Wind velocity measurements using sonic techniques". In: *Bull. Amer. Meteorol. Soc* 45.57, p. 580.

Kossmann, M. et al. (1998). "Aspects of the convective boundary layer structure over complex terrain". In: *Atmospheric Environment* 32.7, pp. 1323–1348. ISSN: 1352-2310. DOI: `http://dx.doi.org/10.1016/S1352-2310(97)00271-9`.

Little, C Gordon (1969). "Acoustic methods for the remote probing of the lower atmosphere". In: *Proceedings of the IEEE* 57.4, pp. 571–578.

— (1972a). "On the detectability of fog, cloud, rain and snow by acoustic echo-sounding methods". In: *Journal of the Atmospheric Sciences* 29.4, pp. 748–755.

— (1972b). "Status of remote sensing of the troposphere". In: *Bulletin of the American Meteorological Society* 53.10, pp. 936–949.

McAllister, LG (1968). "Acoustic sounding of the lower troposphere". In: *Journal of Atmospheric and Terrestrial Physics* 30.7, pp. 1439–1440.

Stull, R.B. (1988). *An Introduction to Boundary Layer Meteorology*. Atmospheric and Oceanographic Sciences Library. Springer Netherlands. ISBN: 9789027727695.

— (2005). *Meteorology For Scientists And Engineers*. Brooks/Cole. ISBN: 9780534408022.

Sun, Wen-Yih and Oliver M. Sun (2015). "Bernoulli equation and flow over a mountain". In: *Geoscience Letters* 2.1, p. 7. ISSN: 2196-4092. DOI: `10.1186/s40562-015-0024-1`.

Tyndall, John (1874). "On the Atmosphere as a Vehicle of Sound". In: *Philosophical Transactions of the Royal Society of London* 164, pp. 183–244. ISSN: 02610523.

Walley, Jerilyn (2013). "Valley Circulation Experiment: A Classification of Wind Flow in the H. J. Andrews Experimental Forest". In:

Appendix A
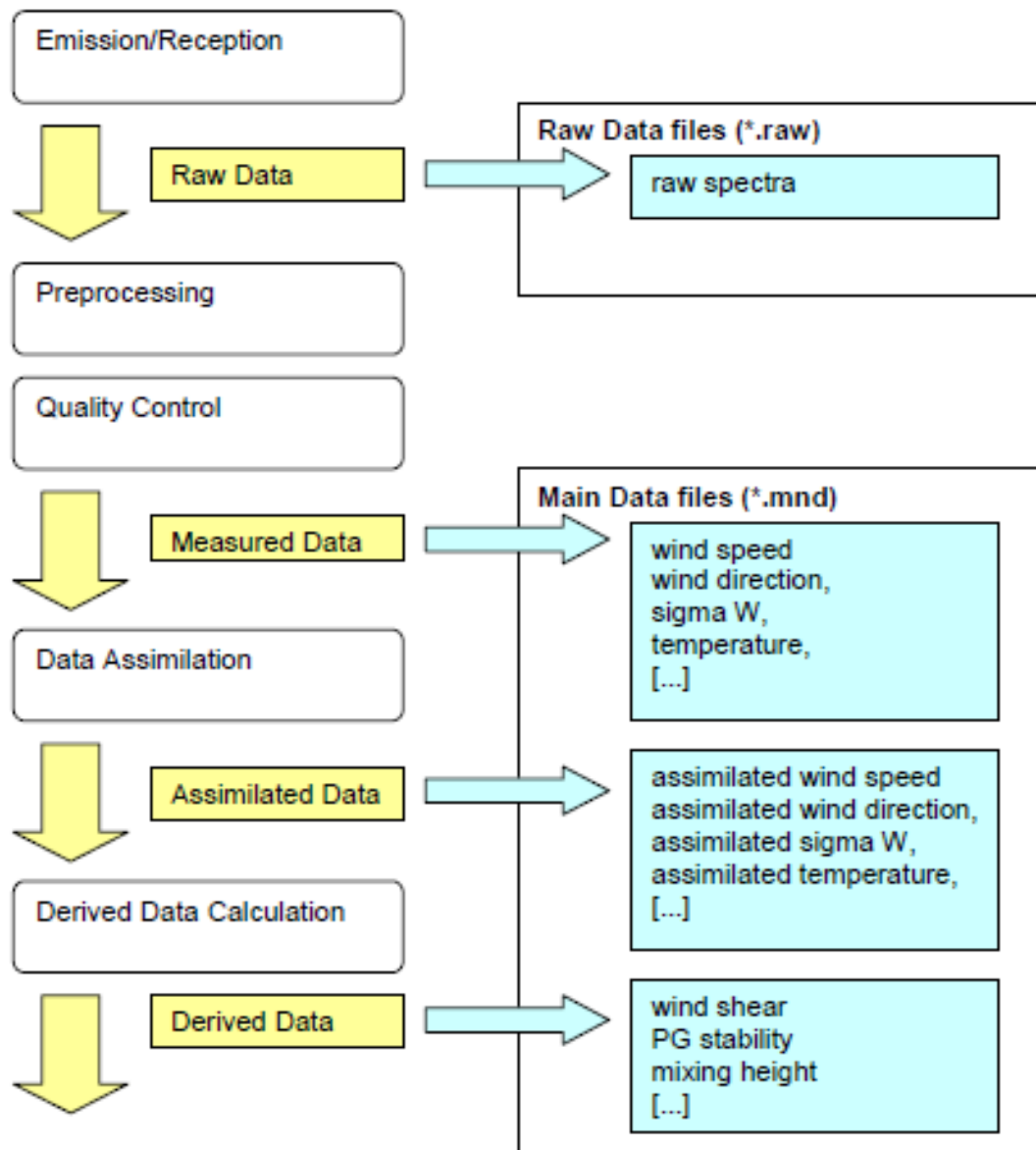
Figure 4.1: Scheme of data flow(AG, 2016)

Appendix B

Table 4.1: Statistic overview 80 [m]

Variable 80 [m]	Min Day	Min Night	Mean Day	Mean Night	Max Day	Max Night
Direction [°]	2.6	0.1	233.9288	241.8764	358	359.8
Velocity [ms^{-1}]	0.27	0.08	6.179654	5.75196	14.51	16.39
σ_W [ms^{-1}]	0.09	0.09	0.4441283	0.2158413	1.51	0.75

Table 4.2: statistic overview 100 [m]

Variable 100 [m]	Min Day	Min Night	Mean Day	Mean Night	Max Day	Max Night
Direction [°]	0.3	0	232.0143	237.4059	355.7	359.7
Velocity [ms^{-1}]	0.19	0.06	7.301664	8.034437	17.21	18.37
σ_W[ms^{-1}]	0.12	0.09	0.5454418	0.3013128	1.81	1.2

Table 4.3: statistic overview 150 [m]

Variable 150 [m]	Min Day	Min Night	Mean Day	Mean Night	Max Day	Max Night
Direction [°]	3	0.5	234.7504	243.5789	358.2	359.1
Velocity [ms^{-1}]	0.3	0.21	7.556271	8.020874	19.89	21.3
σ_W[ms^{-1}]	0.14	0.1	0.6899641	0.3585553	1.93	1.65

Table 4.4: statistic overview 200 [m]

Variable 200 [m]	Min Day	Min Night	Mean Day	Mean Night	Max Day	Max Night
Direction [°]	3.2	0.2	234.3496	248.1058	356.1	359.2
Velocity [ms^{-1}]	0.13	0.38	7.374463	7.007504	17.76	18.75
σ_W[ms^{-1}]	0.14	0.12	0.793734	0.3791667	1.95	1.55

Table 4.5: statistic overview 250 [m]

Variable 250 [m]	Min Day	Min Night	Mean Day	Mean Night	Max Day	Max Night
Direction [°]	0.6	1.2	231.9553	238.5462	357.4	355
Velocity [ms^{-1}]	0.38	0.53	7.390731	6.924401	19.21	19.71
σ_W[ms^{-1}]	0.22	0.11	0.8930696	0.3985514	2.09	1.89

Table 4.6: Occurences of saturated relative humidity (rh>90 [%])

	Day	Night
1	0	18
2	30	0
3	4	42
4	0	65
5	0	0
6	5	44
7	0	0
8	0	0
9	7	25
10	0	0
11	0	0
12	14	36
13	3	54
14	36	13
15	0	0
16	16	34
17	2	20
18	0	0
19	0	0
20	31	1
21	0	23
22	45	0
23	36	46
24	2	19
25	55	11
26	25	67
27	0	20
28	6	12
29	0	36
30	28	10
31	8	36
32	25	0
33	34	0
34	0	53
35	NA	NA
36	60	14
37	6	61
38	0	0
39	0	0
40	21	46
41	15	11
42	NA	4

Table 4.7: Table of classification of Cases - Day

Day	Dir-Y	Dir-N		vel-s	vel-w		dif-h	dif-l		Case
1	26	20	Mix	35	11	S	5	30	L	MS L
2	38	3	Y	41	0	S	1	27	L	Y SL
3	48	0	Y	44	4	S	9	30	L	Y S L
4	44	3	Y	0	47	W	11	31	L	Y S L
5	43	4	Y	45	2	W	3	18	L	Y S L
6	48	0	Y	48	0	S	5	6	Mix	Y S M
7	43	4	Y	15	32	W	7	33	L	Y W L
8	21	25	Mix	34	12	S	6	25	L	M S L
9	48	0	Y	47	1	S	8	29	L	Y S L
10	1	47	N	6	42	W	16	26	Mix	N W M
11	45	3	Y	47	1	S	1	20	L	Y S L
12	46	0	Y	11	35	W	11	32	L	Y W L
13	12	2	Mix	4	10	Mix	4	10	Mix	M M M
14	28	3	Y	11	20	Mix	8	21	L	Y M L
15	27	8	Y	23	12	Mix	3	14	L	Y M L
16	2	6	N	5	3	Mix	0	5	L	N M L
17	33	14	Y	21	26	W	6	37	L	Y W L
18	13	33	N	0	46	W	40	2	H	N W H
19	14	34	N	0	48	W	29	16	Mix	N W M
20	10	28	N	11	27	W	4	29	L	N W L
21	0	45	N	6	39	W	11	28	L	N W L
22	5	37	N	1	41	W	17	6	H	N W H
23	1	32	N	0	33	W	19	9	H	N W H
24	0	1	Mix	0	1	Mix	0	0		MMM
25	26	22	Mix	13	35	W	7	28	L	M W L
26	36	11	Y	5	42	W	11	33	L	Y W L
27	48	0	Y	45	3	S	16	28	Mix	Y S M
28	47	1	Y	35	13	S	8	38	L	Y S L
29	26	20	Mix	22	24	Mix	9	27	L	M M L
30	43	5	Y	20	28	Mix	12	36	L	Y M L
31	24	5	Y	29	0	S	2	12	L	Y S L
32	37	0	Y	37	0	S	2	9	L	Y S L
33	13	22	Mix	28	7	S	5	13	L	M S L
34	44	4	Y	26	22	Mix	8	32	L	Y M L
35	NA	NA		NA	8	S	4	35	L	Y S L
36	47	1	Y	40	3	S	1	27	L	Y S L
37	46	2	Y	45	36	W	16	21	Mix	M W M
38	27	21	Mix	12	35	W	10	30	L	M W L

Table 4.8: Table of classification of Cases - Night

Night	Dir-Y	Dir-N		vel-s	vel-w		dif-h	dif-l		Case
1	11	6	Mix	16	1	S	0	2	L	M S L
2	4	30	N	21	13	Mix	4	7	Mix	N M M
3	34	1	Y	28	7	S	0	13	L	Y S L
4	24	4	Y	20	8	S	1	5	L	Y S L
5	2	23	N	12	13	Mix	4	4	Mix	N M M
6	42	0	Y	42	0	S	0	13	L	Y S L
7	30	7	Y	15	22	Mix	1	1	Mix	Y M M
8	4	8	N	1	11	W	1	0	H	N W H
9	48	0	Y	44	4	S	2	7	L	Y S L
10	14	2	Y	4	12	W	0	2	L	Y W L
11	17	24	Mix	36	5	S	0	3	L	M S L
12	41	6	Y	25	22	Mix	3	34	L	Y M L
13	32	3	Y	5	30	W	5	21	L	Y W L
14	7	1	Y	4	4	Mix	1	4	L	Y M L
15	27	20	Mix	12	35	W	2	17	L	M W L
16	42	4	Y	34	12	S	1	15	L	Y S L
17	3	11	N	0	14	W	3	0	H	N W H
18	0	18	N	0	18	W	13	3	H	N W H
19	7	33	N	28	12	S	1	13	L	N S L
20	23	22	Mix	12	33	W	11	28	L	M W L
21	0	27	N	16	11	Mix	0	0	Mix	N M M
22	3	18	N	2	19	W	7	9	Mix	N W M
23	1	6	N	0	7	W	0	0	Mix	N W M
24	0	10	N	0	10	W	0	1	L	N W L
25	0	20	N	2	18	W	1	3	L	N W L
26	40	1	Y	17	24	Mix	9	12	Mix	Y M M
27	27	11	Y	32	6	S	16	1	H	Y S H
28	42	6	Y	34	14	S	1	16	L	Y H L
29	14	23	Mix	0	37	W	15	13	Mix	M W M
30	33	14	Y	18	29	Mix	4	30	L	Y M L
31	9	16	Mix	7	18	W	5	9	Mix	M W M
32	32	3	Y	34	1	S	0	0	Mix	Y S M
33	37	7	Y	44	0	S	0	2	L	Y S L
34	31	5	Y	13	23	Mix	1	6	L	Y M L
36	30	7	Y	9	28	W	2	23	L	Y W L
37	21	9	Y	19	11	Mix	0	0	Mix	Y M M
38	16	29	Mix	16	29	Mix	16	16	Mix	M M M
39	8	26	N	0	34	W	14	14	Mix	N W M
40	12	6	Y	1	17	W	0	5	L	Y W L